Sadaf Mohtashami

Student ID: 260657567

Expression and proteomic analysis of *KIF1A*/*25B* in hereditary sensory and autonomic neuropathies type II

Laboratory of Dr Guy A. Rouleau

Division of experimental medicine

Faculty of Medicine

McGill University

Montreal, Quebec, Canada

July, 2017

A thesis submitted to McGill University in partial fulfillment of the requirements of the degree of masters in Science.

ABSTRACT

Hereditary sensory and autonomic neuropathies (HSANs) form a group of rare disorders that are characterized by variable sensory and autonomic dysfunctions. HSAN type II (HSAN-II) is a particularly debilitating subtype in which recurrent injuries lead to ulceration, infection, amputation, and death. Despite the significant suffering this disease inflicts, no treatment can yet be offered and much remains to be understood about the pathology underlying HSAN-II. The first cluster of HSAN-II cases was reported in eastern Canada, with half the cases representing patients of French-Canadian descent. This project focuses specifically on answering fundamental questions regarding the molecular pathophysiology of HSAN-II, though the findings could have an important impact on our understanding both of other neuropathies and of normal nerve cell functioning.

Recently the identification of deleterious variations in two genes provided key insights about the genetic architecture and elements underlying HSAN-II. The team of Dr. Guy Rouleau reported truncating mutations in a nervous-tissue-specific exon (HSN2 exon) of the *WNK1* gene (lysine deficient protein kinase 1). The *WNK1* isoform containing the alternatively spliced HSN2 exon was termed the *WNK1/HSN2* isoform, and was found to directly interact with a particular isoform of another HSAN-II causative gene, *KIF1A*. The HSAN-II-causing *KIF1A* isoform is named *KIF1A/25B* as disease-causing mutations were exclusively found in the alternatively spliced exon “25B”. This study focuses on assessing the function of the protein domain encoded by exon 25B through a profiling of its interacting partners; specifically focusing on KIF1A/25B implication in axonal trafficking and slightly investigating the expression profile of KIF1A/25B isoform.

Here, we identified a list of protein interactors of KIF1A/25B through co-immunoprecipitation (co-IP) followed by mass spectrometry. We confirmed KIF1A-SYT11 interaction via co-IP; however, we were unable to confirm that this interaction is unique to exon 25B. SYT11-KIF1A interaction could suggests that KIF1A is a transit system through which SYT11 traffics within the cells and locates at axonal terminal where it plays a role in establishing balanced endo-exocytosis and sustained neurotransmission. Moreover, we found that KIF1A/25B is mainly present in nervous tissue and absent in non-nervous tissues.

RÉSUMÉ

Les neuropathies héréditaires sensitives et autonomiques (HSANs) forment un groupe de maladies rares qui sont caractérisées par un dysfonctionnement des nerfs sensitifs suite à différents processus physiologiques. HSAN de type II (HSAN-II) est un sous-type particulièrement débilitant car lorsque les individus affectés subissent des blessures il est fréquent que celles-ci s'infectent et s'ulcèrent au point de nécessiter des amputations; mettant parfois leur vie en danger. Les premiers cas de HSAN-II ont été rapportés dans l'Est du Canada, la moitié de ceux-ci étaient d'origine Canadienne-Française. Malgré les souffrances importantes associées à cette maladie, aucun traitement n'est encore offert et beaucoup reste à être déterminé au sujet des mécanismes sous-jacents.

Le présent projet vise à apporter des réponses à des questions fondamentales concernant spécifiquement la pathophysiologie moléculaire de HSAN-II; même si ces réponses pourraient aussi avoir un impact important sur la compréhension des autres neuropathies ainsi que sur le fonctionnement normal du système nerveux. Récemment, l'identification de mutations délétères au niveau de deux gènes a permis d'élargir nos connaissances sur HSAN-II. Le groupe du Dr Rouleau a identifié des mutations tronquantes dans un exon spécifique (exon HSN2) d'une isoforme spécifique au système nerveux du gène *WNK1* (protéine kinase 1 déficient en lysine). On réfère à l'isoforme *WNK1* contenant l'exon HSN2 épissé de manière alternative comme étant *WNK1/HSN2*. Le produit du gène *WNK1/HSN2* s'est aussi révélé être un interacteur direct du produit d'un autre gène (KIF1A) dont les mutations causent aussi HSAN-II. Dans ce dernier cas

les mutations délétères sont également dans un exon exclusif (exon 25B) dont l'inclusion est plus abondante dans le système nerveux; on réfère à cette isoforme comme étant *KIF1A/25B*.

Afin d'établir comment l'exon 25B contribue à la maladie, nous avons réalisé un profilage de ses interacteurs protéiques, en se concentrant spécifiquement sur l'implication de KIF1A/25B dans le trafic axonal. Nous avons également fait un premier examen du profil d'expression de l'isoforme KIF1A/25B dans des tissus de souris. Nous avons ainsi identifié une liste d'interacteurs de KIF1A/25B par co-immunoprécipitation (co-IP) suivie de spectrométrie de masse. Une des interactions prometteuses est celle entre KIF1A et SYT11; cependant, nous n'avons pas pu confirmer que cette interaction est unique à l'exon 25B. L'interaction SYT11-KIF1A suggérerait que KIF1A pourrait être un système de transit permettant à SYT11 de passer à l'intérieur des cellules et de se localiser dans les terminaisons axonales où il jouerait un rôle dans l'établissement d'une endo-exocytose équilibrée et d'une neurotransmission soutenue. De plus, nous avons démontré que KIF1A/25B est principalement présent dans les tissus nerveux et est absent des tissus non-nerveux.

TABLE OF CONTENTS

LIST OF FIGURES

LIST OF TABLES

AKNOWLEDGEMENT

First and foremost, I would like to express my sincere appreciation to my supervisor, Dr. Guy Rouleau, for giving me the chance to pursue my graduate studies in his lab. I am grateful for his trust in my abilities to advance the project, his encouragements throughout the journey and his unconditional support regarding the provision of laboratory resources. I would also like to thank my co-supervisor, Dr. Patrick Dion, for his continuous assistance throughout my studies. Dr. Dion has always addressed my concerns about the project, answered my questions and reviewed my writings. Undoubtedly, Dr. Dion had an important impact on my development as a scientist. As well, special thanks to my advisory committee members Dr. Elena Torban and Dr. Geoffrey Hendy for leading the committee meetings.

Furthermore, I am particularly grateful for the support given by Daniel Rochefort and Dr. Jean-François Schmouth for teaching me a wide variety of laboratory techniques. I would like to extend special thanks to Éric Bonneil at the Institute for Research in Immunology and Cancer (IRIC) for guiding me through mass spectrometry analysis.

Last, but not least, I am forever grateful to my parents, Hossein Mohtashami and Azar Bayat, and my supportive sisters for never doubting my capability. Thank you all for being a permanent source of support. Finally, a special thanks to my devoted partner, Dr. Soheil Jamshidi, whose emotional support helped me to pursue the challenging and unpredictable path of basic science research.

PREFACE AND CONTRIBUTION OF AUTHORS

This Master thesis was entirely written by Sadaf Mohtashami and subsequently edited by Dr. Patrick Dion. The mass spectrometry analysis of KIF1A/25B immunoprecipitated samples was done with Éric Bonneil at the proteomic platform of the Institute for Research in Immunology and Cancer (IRIC) at Université de Montréal.

CHAPTER 1: GENERAL INTRODUCTION

1.1 CLINICAL ASPECTS AND PATHOLOGY

1.1.1 Inherited Neuropathies

Inherited neuropathies are a clinically and genetically heterogeneous group of disorders that affect the peripheral nervous system, including motor, sensory, and autonomic fiber types. These inherited neuropathies can be classified into three distinct groups depending on the involvement of the motor or sensory peripheral nervous system (PNS), electrophysiological characteristics, inheritance pattern and genetic variations. These three groups are: 1) hereditary motor and sensory neuropathies (HMSN), also called Charcot-Marie-Tooth, which form the most common type of inherited neuropathies with an incidence of 1 in 2,500 persons; 2) hereditary motor neuropathies (HMN), also referred to as distal spinal muscular atrophies (dSMA); and 3) hereditary sensory and autonomic neuropathies (HSANs) which are the subject of this thesis[1-3].

The clinical similarities among different neuropathies and within one group of neuropathy lead to difficulties in making diagnosis based on clinical findings alone; therefore, it is required to rely on genetic testing, nerve and skin biopsy, and electrophysiological testing to ensure the correct diagnosis[1]. Unfortunately, no specific therapy is currently available for patients affected with these inherited neuropathies. Genetic research of neuropathies has been key in increasing our understanding of the pathogenic events affecting the peripheral nervous system and this knowledge can ultimately unveil much needed therapeutic approaches.

The following section elaborates on hereditary sensory and autonomic neuropathies for which causative genes have been identified to cause nociception and autonomic dysfunctions.

1.1.2 Indifference to pain versus insensitivity to pain

HSANs are associated with nociception defects and autonomic dysfunction. Nociception is the ability to feel pain upon stimulation of a sensory receptor and is a result of four physiological processes: transduction, transmission, modulation and perception[4]. There is a spectrum of anomalous responses in congenital lack of pain sensation; "congenital general pure analgesia"[5], "congenital universal insensitiveness to pain"[6], "congenital universal indifference to pain"[7], and "congenital absence of pain"[8].

Pain insensitivity and indifference to pain are not equivalent; they differ in three aspects[9,10]. 1) Failure to receive stimuli or failure to react to stimuli; insensitivity means a failure to receive and perceive a stimulus while indifference means a lack of concern or reaction to a stimulus received; the distinction between these two terms was introduced for the first time in 1970 by Jewesbury[9]. 2) The presence or absence of peripheral neuropathy; insensitivity to pain is often associated with a neuropathy while indifference to pain is not[10-13]. Patients with congenital indifference to pain have normal peripheral responses to pain but do not sense it; they have painless injuries and experience no other sensory dysfunctions[14,15]. 3) In the case of indifference to pain, nerve fibers, nerve conduction velocities, and axonal reflex are normal while this is not the case for

insensitivity to pain. The inheritance pattern of indifference to pain can be either autosomal dominant or autosomal recessive; although only a few cases have actually been reported[12,14,16,17]. Considering these three aspects that distinguish pain insensitivity from indifference to pain, HSANs are considered to be pain insensitivity disorders.

Defects in sensory pathways (such as NGF/Trk-A signalling) have been considered to be the disease mechanism of insensitivity to pain in HSAN; however, these pathways are intact in individuals showing indifference to pain[9,12]. Most proteins encoded by genes that are mutated in HSANs or HSAN-like phenotypes appear to be linked to various forms of intracellular and endocytic signalling or transmission pathways[4,3].

1.1.3 Hereditary sensory and autonomic neuropathies (HSANs)

A hereditary sensory and autonomic neuropathy (HSAN) was first described in 1968[18]. It was found to be distinct from the other two neuropathies (hereditary motor and sensory neuropathy (HMSN) and hereditary motor neuropathy (HMN)) using three clinical features: 1) mandelian inheritance, 2) involvement of peripheral primary sensory plus or minus autonomic neurons (axons), 3) atrophy of affected neurons (axons).

HSANs form a heterogeneous group of rare disorders characterized mainly by variable sensory and autonomic dysfunction due to peripheral nerve involvement, although motor impairment occurs in many patients[19]. The sensory loss can lead to severe complications, including depressed reflexes, distal sensory loss, recurrent injuries, osteomyelitis[20]. Altered pain and temperature perception leads to ulceration of feet and

hands, mutilation and amputations[21]. Autonomic disturbance may lead to gastroesophageal reflux, syncope, arrhythmia, constipation and anhidrosis (absence of sweeting)[21]. The degeneration of motor neurons leads to shrinkage and weakness of distal limb muscles. Reduced sensitivity to sound may also be present[21].

HSANs are clinically heterogeneous; the severity of the symptoms is variable between different patients and even within a family[22]. The most severe case involves the central nervous system and may lead to mental retardation and premature death. The clinical variations observed in patients affected by an HSAN can be explained by the fact that the aetiology of HSANs pathology is genetically heterogeneous; many genes have been identified to cause this disorder.

There are currently eight types of HSANs, all of which differ based on pattern of dysfunctions, age of onset, autonomic functions, inheritance pattern and predominant clinical features (electrophysiology, nerve biopsy, motor involvement, etc.)[1,10,20,23] (Table 1.1)[4,24]. The subtypes range from autosomal dominant with marked sensory involvement, variable motor involvement and minimal autonomic involvement to autosomal recessive neuropathies that are predominantly autonomic. The estimated incidence of HSANs is about 1 in 25,000[20,25-27]. Only in about 20% of HSAN cases, the causative gene is known and in the remaining 80% the mutated gene have not yet been identified[28]. The following section elaborates on eight types of HSANs that are classified based on their inheritance pattern and causative genes. Figure 1.1 illustrates the location and the function of the proteins encoded by genes associated with all different types of HSAN disorder[21].

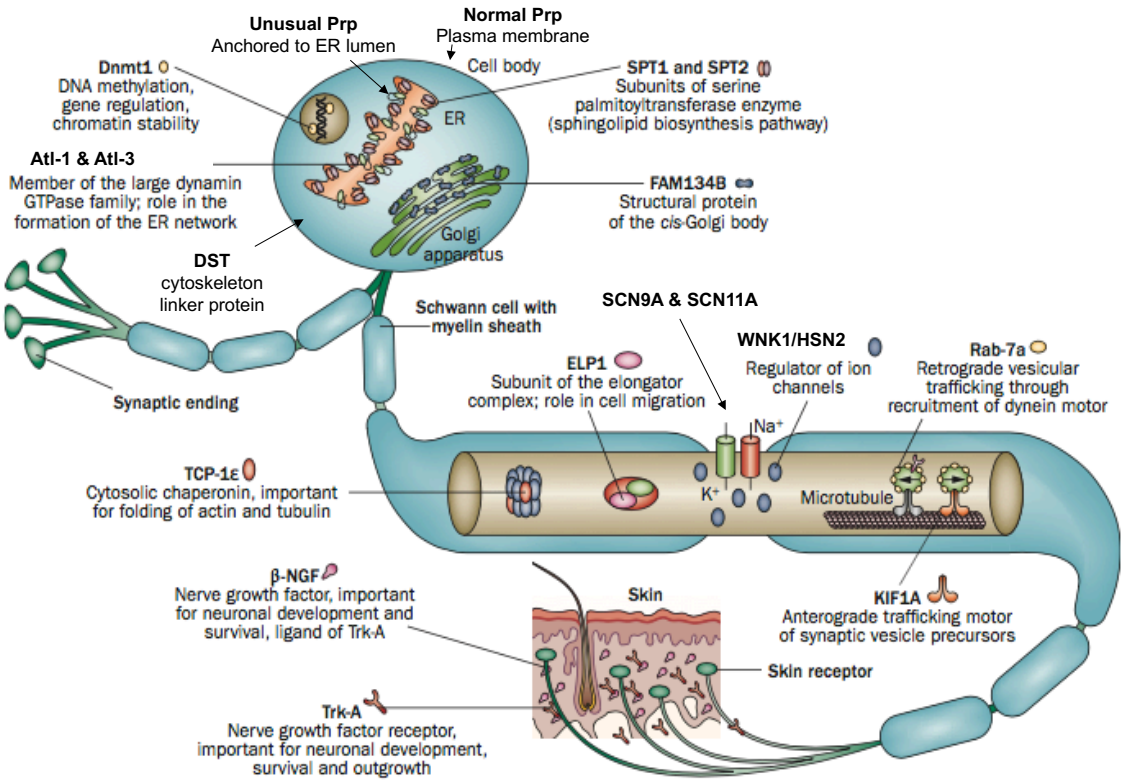

Figure 1.1 : The location and the function of the proteins associated with different types of HSAN[21,29-31].

NGF-β: external cell environment, signal transduction; Trk-A (encoded by *NTRK1*): receptor protein, signal transduction; KIF1A: cytoplasm, anterograde axonal transportation, vesical transportation and neurogenesis; RAB7a: Golgi network, vesicle trafficking; WNK1/HSN 2: axon, ion permeability; SCN9A & SCN11A: transmembrane, potential building; ELP1(encoded by *IKABKAP*): cytoplasm, elongator complex; FAM134B: *cis*-Golgi network, unknown; SPT1 and SPT2 (encoded by *SPTLC1* and *SPTLC2*): Golgi network, sphingolipid synthesis; Prion: cell membrane if normal and ER lumen if unusual; signal transduction (also involved in protection against apoptotic and oxidative stress, cellular uptake or binding of copper ions, formation and maintenance of synapses, and adhesion to the extracellular matrix[32]); DNMT1: nucleus, DNA methylation; ATL1 and ATL3: ER and Golgi apparatus, vesicle trafficking and morphogenesis; DST: cytoplasm, cytoskeleton formation and vesicle transportation; TCP-1ε (encoded by

CCT5): cytoplasm, actin and tubulin folding. The figure is adapted from “Mechanisms of disease in hereditary sensory and autonomic neuropathies” by A. Rotthier *et al*., 2012, *Nat Rev Neurol* **8**, 73-85.

1.1.3.1 Hereditary sensory and autonomic neuropathy type I (HSAN-I)

Hereditary sensory and autonomic neuropathy type I (HSAN-I), also known as hereditary sensory neuropathy (HSN), is the most frequent subtype of HSAN that progresses slowly over time. Its mode of inheritance is autosomal dominant and it manifests in adulthood; between the second and the fifth decades of life[21]. The clinical features of HSAN-I begin with loss of pain and temperature sensation in the lower extremities due to distal sensory loss. Touch and pressure may deteriorate and degeneration of motor neurons may also be present[21,22,26]. Autonomic involvement is absent or weak. Ulcers on the extremities are common, which may lead to amputation and painless injuries[33-35]. So far, mutations in six genes are associated with the development of HSAN-I: *SPTLC1* [MIM 605712], *SPTLC2* [MIM 605713]*, ATL3* [MIM 609369], *ATL1* [MIM 606439], *DNMT1* [MIM 126375] and *RAB7* [MIM 602298].

SPTLC1 encodes one of the three subunits of serine palmitoyltransferase (SPT); it is located on the long (q) arm of chromosome 9 at position 22.31 (9q22.31) and consists of 15 exons. *SPTLC2* encodes the other subunit of serine palmitoyltransferase (SPT); it is located on the long (q) arm of chromosome 14 at position 24.3 (14q24.3) and consists of 12 exons[21,35-39]. *SPTLC2* is not a common cause of HSAN-I[40]. Serine palmitoyltransferase (SPT) is an acyltransferase enzyme located on the endoplasmic

reticulum (ER) and plays an important role in the rate limiting step of sphingolipid biosynthesis[41,42]. Sphignolipids are the key components of the cell membrane and play a crucial role in signal transduction and membrane trafficking[21,42,43]. In HSAN-I patients, gain of function mutations of *SPTLC1* and *SPTLC2* result in the formation of two abnormal sphingolipid metabolites that have toxic effect on neurons; they interfere with the formation of neurites[44]. *In vitro* studies show that sensory neurons are more impaired by these atypical metabolites than motor neurons[44].

Atlastin GTPase 3 (*ATL3*) is another gene mutated in affected HSAN-I patients[45]. This gene is located on the long arm (q) of chromosome 11 at position 13.1 (11-q13.1). Whole exome sequencing of three affected families led to the identification of two missense mutations (p.Tyr192Cys and p.Pro338Arg) in atlastin GTPase 3. Another GTPase involved with the development of HSAN-I is atlastin-1 (ATL1); three missense mutations in *ATL1* (p.Asn355Lys, p.Glu66Gln and p.Val326TrpfsX8) were identified in HSAN-I patients. *ATL1* gene is located on the long arm (q) of chromosome 14 at position 22.1 (14-q22.1). It encodes the large dynamin-related GTPase atlastin-1 and it is known to be mutated in early-onset hereditary spastic paraplegia (SPG3A) as well.

The atlastins are a family of integral membrane GTPases located on the tubular endoplasmic reticulum[45-47]. They help the formation of three-way junctions that connect tubules in ER; therefore, they are required for proper ER network formation[48,49]. The missense mutation in *ATL3* (p.Tyr192Cys) leads to displacement of *ATL3* and overexpression of this mutation leads to changes in the morphology of three-way junctions and endoplasmic reticulum[46]. ATL-1 mutations in HSAN-I patients lead to

reduced activity of atlastin-1 GTPase and change in the morphology of endoplasmic reticulum[50].

Another gene associated with HSAN-I pathology is DNA methyltransferase 1 (*DNMT1*) located on the short arm (p) of chromosome 19 at position 13.2 (19p13.2). *DNMT1* encodes an enzyme responsible for propagation of methyl groups (epigenetic marks) to daughter somatic cells after replication. Therefore, DNMT1 plays a role in gene regulation and chromatin stability[51-60]. DNA methylation is responsible for neurogenesis, repairing DNA mismatch, and regulating neural cell-cycles, development, survival and connectivity[52,61-63]. Mutated DNMT1 proteins become degraded prematurely and will not be able to interact with heterochromatin; this leads to reduced methyltransferase activity and deregulation of genome methylation levels[51]. It has been shown that mouse embryonic stem cells that express mutated DNMT1 protein are more prone to undergo apoptosis and fail to differentiate to neuronal lineage[55]. It has also been shown that *DNMT1* mutations are responsible for a specific type of HSAN-I[64,65] in which both central and peripheral neurons become degenerated leading to dementia and hearing loss.

A rare subtype of HSAN-I, called HSAN-IB, has been described to have an adult onset of cough and gastroesophageal reflux. The gene causing this disorder is located on the short arm (p) of chromosome 3 at position (3p22-24); however, the name of the gene and its function remain to be identified[66,67].

1.1.3.2 Hereditary sensory and autonomic neuropathy type II (HSAN-II)

This study focuses mainly on HSAN-II; although the findings could have an important impact on our understanding both of other neuropathies and of normal nerve cell functioning. HSAN-II is a rare autosomal recessive disorder defined by progressive degeneration of peripheral neurons with onset in the first decade of life[68-71]. There are two different clinical subtypes within HSAN-II: a stable congenital form that is non-progressive as well as a progressive one[72,73].

HSAN-II was initially described in 1973 in French-Canadians[70]. HSAN-II is also called "neurogenic acro-osteolysis", "hereditary sensory radicular neuropathy" or "congenital sensory neuropathy"[74]. It is characterized by loss of perception to pain, touch, and heat due to a loss of peripheral sensory nerves. Distal pathology (paronychia, ulcers and necrosis, Charcot joints, unrecognized burns or fractures, amputations) are due to the loss of all modalities of sensation in lower and upper limbs as well as truncal involvement in severe cases. Primarily distal sensory loss affects the lower limbs most severely. Abnormalities in the sensation of discriminative touch and pressure are most common. Pain insensitivity (no reaction to pinprick or strong compression) is observed at varying levels; complete loss is also possible. The lack of pain perception results in ulcerations, self-mutilations, painless fractures and joint injuries[2,74,75].

On examination, there is an absence or reduction of tendon reflexes, minimal autonomic dysfunction, absence of sensory nerve action potentials (SNAPs) and elevated vibratory and thermal thresholds[72]. Biopsies of the sural nerve from HSAN-II patients show a reduction in axon caliber and virtually complete depletion of all myelinated fibers

due to Wallerian-like axonal degeneration and a reduction in the number of unmyelinated fibers as well as segmental demyelination[4,76,77]. Despite the significant suffering this disease inflicts, no treatment can yet be offered and much remains to be understood about the pathology underlying HSAN-II. The causative genes of HSAN-II that are known so far are discussed in section 1.2 (Genetics of HSAN-II).

1.1.3.3 Hereditary sensory and autonomic neuropathy type III (HSAN-III)

Hereditary sensory and autonomic neuropathy type III (HSAN-III), also known as familial dysautonomia (FD) and Riley-Day syndrome, is a recessive neuropathy that manifests in infancy[78,79]. HSAN-III manifests in decreased pain and temperature sensation, depressed tendon reflexes with extensive autonomic dysfunction. Autonomic disturbances include the inability to secrete tears, excessive sweating, gastrointestinal dysmotility and vasomotor and cardiovascular perturbations[21,80-82]. Self-mutilation is less common than in other types of HSANs. The lifespan of an HSAN-III patient is greatly reduced; only 50 percent of affected patients reach the age of 40 and affected individuals die due to renal or pulmonary failure[21,80-83].

Mutation in the *IKBKAP* gene is responsible for HSAN-III and three specific point mutations (loss of function) have been identified[25,82-84]. The *IKABKAP* gene is located on the long (q) arm of chromosome 9 at position 31.3 (9q31.3) and includes 37 exons. The *IKABKAP* gene encodes for I-k-B kinase complex associated protein, also called elongation protein 1 (ELP-1). Mutation in this gene leads to production of truncated

IKBKAP mRNA and reduction in IKAP protein which mostly affect the sensory and autonomic neurons. The expression of truncated and wild type IKBKAP is tissue specific[82,85]. It has been shown that both gain and loss of function mutations in the *IKABKAP* gene impair neuronal polarity, differentiation and survival suggesting the pleotropic role of *IKABKAP* gene in both the peripheral and central nervous system[86]. It has been also shown that *IKABKAP* encodes the largest subunit of RNA Polymerase II Elongator Complex which is required for elongation of many genes during transcription[87].

The mouse model of HSAN-III with homozygous mutations on the *IKABKAP* gene shows developmental delay, cardiovascular defects and early embryonic lethality; this suggests that *IKABKAP* gene is crucial for the expression of the genes involved in cardiac morphogenesis and embryonic lethality is the result of cardiac failure[88,89].

1.1.3.4 Hereditary sensory and autonomic neuropathy type-IV (HSAN-IV)

Hereditary sensory and autonomic neuropathy type IV (HSAN-IV) is an autosomal recessive neuropathy that manifests in infancy or early childhood. HSAN-IV is a very rare type of HSAN that involves both pain insensitivity and autonomic defects. HSAN-IV is also known as congenital insensitivity to pain with anhidrosis (inability to perspire), CIPA. The sensation of pain is abnormal, but touch and pressure are unaffected. Painless injuries and self-mutilations are frequent.[90] HSAN-IV is characterized by varying level of intellectual disability and increased risk of ortheopaedic complications like fracture, osteomyelitis, avascular necrosis, Charcot joints and joint instability[91-94].

The loss of function mutations in *NTRK1* gene, also known as *TRK-A*, is responsible for the development of HSAN-IV disorder[95-97]; this explains that NGF/TRK-A pathway is responsible for this disorder. *NTRK1* gene is located on the long arm (q) of chromosome 1 at position 23.1 (1q23.1) and encodes for the high-affinity tyrosine kinase receptor I for Neurotrophic Growth Factor (NGF)[98,99]. Its single transmembrane domain divides the protein into an intracellular domain that is responsible for signaling and an extracellular domain that binds to NGF[100]. Three missense mutations and two nonsense mutations are identified as HSAN-IV causative mutations on the NTRK1 gene; these mutations are present in various domains of NTRK1 that bind to NGF. Interaction between NGF and TRK-A is required for the survival and maintenance of NGF-dependent neurons; therefore, patients affected with HSAN-IV lack all NGF-dependent neurons: primary afferent and sympathetic postganglionic neurons[101-103]. The lack of primary afferent neurons lead to pain insensitivity and the lack of sympathetic postganglionic neurons leads to anhidrosis[91,95]. Defective thermoregulation and anhidrosis in HSAN-IV patients is fatal in up to 20% of patients before the age of three years[93,104]. In order to treat the orthopaedic complications, arthrodesis, corrective osteotomy, and limb-lengthening procedures are performed[93,94].

1.1.3.5 Hereditary sensory and autonomic neuropathy type V (HSAN-V)

Hereditary sensory and autonomic neuropathy type V (HSAN-V) is an autosomal recessive disorder, also known as Norrbottnian congenital insensitivity to pain [74,105,106]. It is characterized with pain and temperature insensitivity that results in painless burns,

fractures and ulcerations. No other sensory components are affected and most other neurological functions like mental ability and sweating are intact[107]. Neurophysiological studies show reduction of both unmyelinated and myelinated nerve fibers[107].

Two mutations in the human nerve growth factor beta (*NGF-B*) gene have been identified as causative genes of HSAN-V: R211W and 681delGG[21,108]. The *NGF-B* is located on the short arm (p) of chromosome 1 at position 13.2 (1p13.2). It encodes the NGF protein and plays an important role in sympathetic axon growth and survival[109]. Dysfunction in the NGF system is responsible for the development of both HSAN-V and HSAN-IV[106]. Since intellectual disability is absent in HSAN-V patients, these NGF mutations do not interfere with the role of NGF in the development of the central nervous system. However, they interfere with the peripheral pain pathway[107].

HSAN-V is the least common type of HSAN; only a few cases have been reported and the molecular basis and the phenotypic description of this disorder is not well understood[19,74,107,110-112]. Knockout mice models for NGF and TRK-A show impaired nociceptive function and the crucial role of these molecules in the peripheral and central nervous systems' development[106,113,114].

1.1.3.6 Hereditary sensory and autonomic neuropathy type VI (HSAN-VI)

HSAN-VI, an autosomal recessive disorder, was first diagnosed in four affected infants of an Ashkenazi Jewish family. The phenotypic features are very similar to that of HSAN-III (FD) but more severe and accompanied by distal arthrogryposis (joint

contractures). Patients suffer from neonatal hypotonia, respiratory and feeding difficulties, absence of tearing and motionless open-mouthed facies[115]. Frame shit mutations in *DST* gene is the cause of this pathology[115-117]. This gene is located on the short arm (p) of chromosome 6 at position 12.1 (6p12.1); it gene encodes dystonin that link actin filaments to microtubules. Dystonin is required for maintaining neuronal cytoskeleton organization and vesicle trafficking and mutated dystonin interfere with proper development of peripheral nerves[115,117].

1.1.3.7 Hereditary sensory and autonomic neuropathy type VII (HSAN-VII)

HSAN-VII is an autosomal dominant disorder characterized by pain insensitivity, self-mutilations and painless fractures. Mutation in *SCN11A* gene is the cause of this pathology[118,119]. This gene is located on the short arm (p) of chromosome 3 at position 22.2 (3p22.2). *SCN11A* encodes voltage-gated sodium ion channels that are essential for the generation of action potentials and thus the proper functioning of nociceptors. Nociceptors are neurons that transmit sensory information from the body periphery to the central nervous system (spinal cord) and detect pain; *SCN11A* is highly expressed in nociceptive neurons of the dorsal root ganglia (DRG) and trigeminal ganglia[120,121]. Mutation in *SCN11A* leads to excessive activity at resting voltages, depolarization of nociceptors, impaired generation of action potentials and abnormal synaptic transmission[118].

1.1.3.8 Hereditary sensory and autonomic neuropathy type V-III (HSAN-VIII)

Recently mutations in the *PRDM12* gene were proposed to be the cause of another type of HSAN: HSAN-VIII, an autosomal recessive disorder[30,122]. *PRDM12* belongs to a family of epigenetic regulators that control neural specification and neurogenesis[123]. It is expressed in nociceptors and their progenitors and plays a crucial role in pain perception. It has been suggested that mutations in the *PRDM12* gene cause developmental defects in the sensory neurons that are destined to become nociceptors[124]. *PRDM12* gene is located on the long arm (q) of chromosome 9 at position 34.12 (9q34.12).

Truncation mutations in *PRNP* gene that encodes the prion protein leads to a specific type of hereditary sensory and autonomic neuropathy characterized by chronic diarrhea, nausea, autonomic failure, neurogenic bladder and urinary tract infections[30,125]. This type of HSAN manifests in adulthood (4th decade of life) and it has an autosomal dominant mode of inheritance[126]. The cellular prion protein is localized on the cell surface and in different organs but is also highly expressed in the central and peripheral nervous systems[127]. When misfolded, prion protein aggregates in the cytoplasm of cells in the central nervous system, peripheral nerves, skeletal muscle, skin and internal organs causing cell death[29]. This leads to defective signal transduction leading to diarrhea, autonomic failure and neuropathy.

A very rare case of hereditary sensory and autonomic neuropathy is accompanied by spastic paraplegia[128]. Its mode of inheritance can be either autosomal dominant or autosomal recessive. Mutation of the *CCT5* gene that encodes the epsilon subunit of the

cytosolic chaperonin-containing t-complex peptide-1 (TCP-1ε) is responsible for this pathology[30,129]. CCT5 is required for the actin and tubulin folding in the cytosol[130].

1.2 GENETICS OF HSAN-II

The first cluster of HSAN-II cases was reported in eastern Canada and more than 50% of patients were of French-Canadian origin[70,131,131-135]. HSAN-II is genetically heterogeneous and it is classified in four groups according to the gene causing it: HSAN-IIA (***WNK1/HSN2***)[2], HSAN-IIB (***FAM134B***)[75], HSAN-IIC (***KIF1A***)[136,137] and more recently HSAN-IID (***SCN9A***)[138]. Despite rapid identification of HSAN-II genes, the etiology of many cases remains unexplained[28].

1.2.1 HSAN-IIA (***WNK1/HSN2***)

In 2004, the team of Dr. Guy Rouleau found three different truncating mutations in five affected HSAN-II families from an isolated population living in Newfoundland and rural Quebec[74]. The team proposed that these mutations were positioned in a conserved single-exon ORF (open reading frame) of a novel gene named *HSN2* and that mutation of this ORF was the cause of HSAN-II pathology[74]. However, this *HSN2* gene appeared to be lying within the intron 8 of a larger gene (*PRKWNK1: lysine deficient protein kinase 1*). Subsequently, upon screening a HSAN-II Lebanese family, the team found an additional 1bp deletion mutation in the *HSN2* gene. Following this discovery, other *HSN2* mutations were reported in patients of different origins[131,139-142]. At that point *WNK1*

mutations were only known to be intronic deletions causing Gordon hyperkalemia-hypertension syndrome[143].

Later, the identification of compound heterozygous mutations in *HSN2* and exon 6 of *WNK1* revealed that *HSN2* is not an independent single exon gene but a nervous-tissue-specific exon of *WNK1*[2]. This has been the only report of compound heterozygous mutations in *HSAN2*[2]. In fact, *HSN2* is an alternative *WNK1*-spliced exon that is located between exon 8 and exon 9 of the nervous system *WNK1* isoform variant 4; this particular isoform is referred to as *WNK1/HSN2* isoform[136,137]. This isoform is located on the short arm (p) of chromosome 12 at position 13.33 (12p13.33)[74]. Expression profile studies of *WNK1/HSN2* shows that it is expressed in both the cell body and axon while *WNK1* is only expressed in the cell body and not in axons[2]. Also, *WNK1/HSN2* is more abundant in sensory neurons compared to motor neurons; this finding may explain the role of *WNK1/HSN2* mutation in the sensory loss phenotype of HSAN-II[2]. At least twelve mutations have been reported to cause HSANII-A [2,74,131,140-142,144,145].

1.2.2 HSAN-IIB (***FAM134B/RAB7***)

Shortly after the *WNK1/HSN2* report, an independent group of researchers screened a consanguineous Saudi Arabian family affected by HSAN-II. The screening showed no mutations in *WNK1/HSN2*; however, it revealed truncating mutation in *FAM134B* (also called JK-1) gene located on the short arm (p) of chromosome 5 at position 15.1 (5p15.1)[75]. *FAM134B* belongs to a family of three genes whose function is

not known: *FAM134A, FAM134B, FAM134C.* In case of *FAM134* knockdown in primary dorsal root ganglion neurons, the structure of *cis*-Golgi apparatus changes and these neurons undergo apoptosis (programmed cell death)[75]. This finding suggests the possible role of FAM134B protein in processing of neurotrophin precursors and the transportation of their receptors because dorsal root ganglion neurons undergo apoptosis in absence of neurotrophin as well[146,147].

RAB7 (Ras-related small GTPase 7) is another causative gene for HSAN-IIB; it is also involved in the development of HSAN-I[26,30,148-150]. This gene is located on the long arm (q) of chromosome 3 at position 21.3 (3q21.3). The Rab proteins play a regulatory role in intracellular vesicular trafficking and late endocytic pathway[151]. It cycles between GTP-bound form (active) and GDP-bound form (inactive); this cycling occurs with the help of guanine exchange factor (GEF) and GTPase-activating protein (GAP)[152-155]. The patients with mutant RAB7 suffer from ulcers and limb-mutilating complications as well as motor fiber degeneration; this lead to a disagreement between scientists as to whether to classify this neuropathy as hereditary sensory & autonomic neuropathies (HSAN) or hereditary motor and sensory neuropathies (HMSN)[26].

1.2.3 HSAN-IIC (***KIF1A***)

Following the identification of the above genes, the team of Dr. Rouleau further focused on HSAN-II disorder and the *HSN2* exon of *WNKI/HSN2*. A yeast two-hybrid screen (Y2H) identified direct protein interactors of the HSN2 region of *WNK1* gene

(*WNKI/HSN2* isoform). At the same time, homozygosity mapping of a consanguineous Afghan family with HSAN-II (*WNK1/HSN2* and *FAM134B* were excluded) identified a candidate interval. This interval contained 38 genes and one was *KIF1A* which was observed to be an interactor of the *WNKI/HSN2* isoform[156]. *KIF1A* gene is located on the long arm (q) of chromosome 2 at position 37.3 (2q37.3). Human *KIF1A* gene has 46 exons and 3 alternatively spliced exons (*13B*, *25B*, & *36B*) [UCSC Genome Browser (GRCh37/hg19)]. Sequencing revealed a 1bp deletion in exon *25B*[156]. Subsequent screening identified the same mutation in unrelated cases from Turkey and Belgium[156]. Similar to *WNK1/HSN2*, every *KIF1A* mutation identified was only within an alternatively spliced exon (*25B*); this particular isoform is referred to as *KIF1A/25B* isoform.

1.2.4 HSAN-IID (***SCN9A***)

Mutations in *SCN9A* is considered to be responsible for the development of HSANII-D[137,138,157]. *SCN9A* is located on the long arm (q) of chromosome 2 at position 24.3 (2q24.3). *SCN9A* encodes the alpha subunit of the voltage-gated sodium ion channels required for the generation of action potentials. *SCN9A* is highly expressed in nociceptive neurons. Initially, the sequence analysis of this gene in three consanguineous families from northern Pakistan and affected by HSAN-II led to the identification of three homozygous nonsense mutations (S459X, I767X and W897X) in *SCN9A* gene. These mutations cause *SCN9A* protein loss of function. Later, another homozygous loss of function mutation (c.3993delGinsTT) was identified in two other HSAN-II affected Japanese families[138].

HSAN-II cases associated with FAM134B and SCN9A mutations have greater autonomic symptoms than cases with WNK1/HSN2 or KIF1A/25B mutations. In the case of FAM134B this observation is coherent with its expression in sensory, autonomic, and central nervous system (CNS) neurons[75].

It's been reported that heme metabolism and intracellular heme levels play an important role for the maintenance of sensory neurons. Next generation sequencing of the DNA extracted from the fibroblast and lymphoblastoid cell lines of the patients suffering from congenital loss of pain perception and without mutation in any of the known genes associated with HSAN showed mutations in the *FLVCR1* (Feline Leukemia Virus subgroup C Receptor 1) gene[158]. The FLVCR1 protein is a heme exporter and this mutation leads to reduced heme export activity, increased oxidative stress and increased sensitivity to programed cell death[158]. *FLVCR1* is also the causative gene of Posterior Column Ataxia and Retinitis Pigmentosa (PCARP)[159].

Moreover, a recent paper that has been accepted for publication identifies a homozygous frame shift mutation in *ARL6IP1* gene (ADPrRibosylation-like factor 6-interacting protein 1) in one patient suffering from congenital insensitivity to pain, sensory neuropathy, self-mutilation, and spastic paraplegia[160]. The ARL6IP1 protein, whose mutant form is non-functional, is one of the interactors of ATL1 GTPase and plays a role in shaping the endoplasmic reticulum.

1.3 RATIONAL AND APPROACH.

KIF1A belongs to the kinesin-related family of proteins; it is a neuron-specific motor that transports organelles towards the plus-end of the microtubules; It is proposed that KIF1A is involved in the transportation of synaptic vesicle precursors[161,162]. Identification of mutations in specific isoform of *KIF1A* (*KIF1A/25B*) in HSAN-II patients may suggest defective axonal transport of synaptic vesicles in these patients. It has been shown that WNK1/HSN2 and KIF1A/25B interact with each other but it remains unclear how the trafficking of WNK1/HSN2 (and possibly of some WNK1/HSN2 interactors) outside of the neuronal cell bodies involves KIF1A/25B[156]. Moreover, we know that WNK1/HSN2 moves out of the cell body to the axons while WNK1 without HSN2 does not[2].

The objective of this thesis is to shed light on the poorly understood nature of the KIF1A/25B isoform by establishing its expression profile across the nervous system and identifying the interacting partners of the protein domain encoded by exon 25B.

To establish the expression profile of *KIF1A/25B* in wild type mice, Western blot (WB) immunodetection and immunofluorescence (IF) assay was performed using tissues from adult wild-type C57BL/6J mice and a rabbit polyclonal antiserum developed in our lab in collaboration with Capralogics laboratory. The antiserum has been raised against a specific peptide sequence of the murine orthologue region encoding exon 25B. The protein lysates are prepared from brain and spinal cord (CNS) and lysates from kidney, liver, and lung tissues are used as controls.

To identify proteins that interact with exon 25B of KIF1A, co- immunoprecipitation

(co-IP) is performed and novel candidate interactors are detected using a liquid chromatography–mass spectrometry (LC-MS) approach.

Establishing the expression profile of KIF1A/25B protein and identifying the proteins that interact with this protein help unraveling the molecular mechanisms that underlie sensory and autonomic neurodegeneration of HSAN-II. This understanding could assist in designing therapeutic strategies for patients with HSAN-II.

Table 1.1: Classification of hereditary sensory and autonomic neuropathies based on their inheritance pattern and causative genes

Clinical type	Inheritance	Locus	Gene	Age at onset
HSAN1A/HSN1A	Autosomal dominant	9q22.1-q22.3	**SPTLC1** (seine palmitoyltransferase long chain subunit 1)	Adolescence
HSAN1B/HSN1B	Autosomal dominant	3p24-p22	?	Adulthood
HSN1C	Autosomal dominant	14q24.3	**SPTLC2** (seine palmitoyltransferase long chain subunit 2), **RAB7** (a member of RAS oncogene family)	Adulthood
HS1D	Autosomal dominant	14-q22.1	**ATL1** (atlastin-1)	Adulthood
HSN1E	Autosomal dominant	19p13.2	**DNMT1** (DNA methyltransferase 1)	Adulthood
HSAN1F	Autosomal dominant	11q13.1	**ATL3** (atlastin-3)	Broad range of age at onset
HSAN2A/HSN2A	Autosomal recessive	12p13.33	**WNK1/HSN2** (protein kinase, lysine-deficient 1)	Childhood
HSAN2B/HMSN2B	Autosomal recessive	5p15.1, 3q21.3	**FAM134B** (family with sequence similarity 134, member B), **RAB7/RAB7A** (a member of RAS oncogene family)	Childhood
HSN2C	Autosomal recessive	2q37.3	**KIF1A** (kinesin, heavy chain, member 1A)	Childhood to adolescence

Clinical type	Inheritance	Locus	Gene	Age at onset
HSAN2D	Autosomal recessive	2q24.3	**SCN9A** (sodium channel voltage-gated type IX)	Childhood
HSAN3	Autosomal recessive	9q31.3	**IKBKAP** (inhibitor of kappa light polypeptide gene enhancer in b cells, kinase complex-associated protein)	Congenital
HSAN4	Autosomal recessive	1q23.1	**NTRK1** (neurotrophic tyrosine kinase, receptor type 1)	Congenital
HSAN5	Autosomal recessive	1p13.2	**NGFB** (nerve growth factor, beta subunit)	Congenital
HSAN6	Autosomal recessive	6p12.1	**DST** (dystonin)	Childhood
HSAN7	Autosomal dominant	3p22.2	**SCN11A** (sodium channel voltage-gated type XI)	Early childhood
HSAN8	Autosomal recessive	9q34.12	**PRDM12** (PR domain-containing protein)	Congenital
HSAN + Diarrhea	Autosomal dominant	20p13	**PRNP** (prion protein)	Adulthood
HSN + Spastic paraplegia	Autosomal dominant/ recessive	5p15.2	**CCT5** (chaperon containing T-complex [polypeptide 1)	Childhood

CHAPTER 2: EXPERIMENTAL METHODS AND RESULTS

2.1. EXPERIMENTAL METHODS

2.1.1 SCREEN FOR PROTEIN INTERACTORS OF KIF1A/25B

2.1.1.1 Eukaryotic DNA expression constructs

I) Full-length KIF1A/25B: The human cDNA corresponding to this protein was obtained from Kazusa DNA Research Institute in Japan (Accession number: AB290172). Primer 1 and 2 (Table 2.1) were used to amplify the ORF of KIF1A/25B cDNA. The mammalian expression vector pCS2 carrying a 6-Myc tag in C-terminal was digested at EcoRI and BamHI digestion site and the KIF1A/25B cDNA was cloned in this vector by Gibson assembly[163]. The sequences were subsequently verified by Sanger sequencing. The cDNA corresponding to full-length KIF1A/25B protein is 5,673 bp which within ORF translates into 1,920 amino acids (MW 217.2 kDa).

II) Full-length KIF1A/25B minus exon 25B: This construct was created using the pCS2 vector expressing full-length KIF1A/25B with 6-Myc in C-terminal. Using PCR, the two fragments on either side of the exon 25B were amplified and joined by Gibson assembly[163]. For each fragment, two primers were used (Table 2.1). The sequences were subsequently verified by Sanger sequencing. The cDNA corresponding to full-length KIF1A/25B minus exon 25B protein is 5,396 bp which within ORF translates into 1,798 amino acids (MW 203.6 kDa).

III) Exon25B alone: This construct was created using pCS2 vector expressing full-length KIF1A/25B with 6-Myc tag in C-terminal. Using primer 7 and 8 (Table 2.1), the region that belongs to the exon 25B was amplified by PCR and joined by Gibson assembly[163]. Sequences were verified by Sanger sequencing. The cDNA corresponding

to exon 25B protein is 283 bp and it translates into 94 amino acids (MW 10.2 kD). In ORF, it contains 579 bp and translated into 192 amino acids (MW 22 kDa).

IV) Enhanced green fluorescent protein (EGFP): The cDNA corresponding to the EGFP was amplified using primer 9 and 10 (Table 2.1). The pCS2 expression vector carrying a 6-Myc tag in C-terminal was digested by BamHI and BsrGI and the cDNA corresponding to the EGFP was cloned in this vector by Gibson assembly[163]. The sequences were verified by Sanger sequencing. The cDNA corresponding to the EGFP protein is 717 bp which within ORF translates into 337 amino acids (MW 38.5 kDa).

V) Synaptotagmin XI: The cDNA corresponding to mouse SYT11 was obtained from the Origen biomedical company and was amplified using primer 11 and 12 (Table 2.1). The pCS2 expression vector carrying a 3-Flag tag in C-terminal was digested by SmaI and SacI and the cDNA corresponding to SYT11 was cloned in this vector by Gibson assembly[163]. The sequences were verified by Sanger sequencing. The cDNA corresponding to SYT11 protein is 1141 bp which within ORF translates to 510 amino acids (MW 57.6 kDa).

Table 2.1: The sequences of primers used for the PCR reaction

Full-length KIF1A/25B	
1) Forward	5'-CGTGGATCCCCGGAATTCCCgATGGCCGGGGCTTCGGTGAA-3'
2) Reverse	5'-GTCACGATGCGGCCGCTCGATCAGACCCGCATCTGGGCAGACC-3'
Full-length KIF1A/25B minus exon 25B	
Fragment 1:	
3) Forward	5'-GCTACTTGTTCTTTTTGCAGGATCCCATACCATGGCC-3'
4) Reverse	5'-TACACGAAGGCACTGCCCACCAGCCGGA-3'
Fragment 2:	
5) Forward	5'-GGTGGGCAGTGCCTTCGTGTACCTGAGCAAC-3'
6) Reverse	5'-CGTAATACGACTCACTATAGTTCTAGAGGCTCGAGAGGC-3'
Exon 25B alone	
7) Forward	5'-TTCTTTTTGCAGGATCCCATaccatgggcAGTTCAGCCATCTCTGGCTG-3'
8) Reverse	5'-CTTTTGCTCCATAGCTTTAAATCTTCCTACTAAACTGAACaGGGGGG-3'
Enhanced green fluorescent protein (EGFP)	
9) Forward	5'-TTCTTTTTGCAGGATCCCATCCACCATGGTGAGCAAGGG-3'
10) Reverse	5'-CTTTTGCTCCATAGCTTTAAATGACTTGTACAGCTCGTCCATGC-3'
Synaptotagmin XI	
11) 5'-GGACTTTCCAAAATGTCG-3'	
12) 5'-ATTAGGACAAGGCTGGTGGG-3'	

The XL10-Gold ultracompetent *Escherichia coli* cells were transformed following Agilent technologies protocol. Lysogeny broth (LB) plates with ampicillin were used to select bacterial colonies carrying the pCS2 expression vector as the later encodes an ampicillin resistance gene. The colonies of resistant cells were picked and grown over night in LB media (37°C while shaking at 220 rpm). DNA was extracted from these bacterial culture using Qiagen DNA extraction kit. The cDNA Sanger sequencing was performed at McGill University and Génome Québec Innovation Centre.

2.1.1.2 Cell lines, culture condition, transfection and protein extraction

The human embryonic kidney cell line (HEK293T) was used in this study. Cell cultures were maintained at 37°C in Dulbecco's modified eagle medium (DMEM) nutrient mixture (life technologies) supplemented with 10% fetal bovine serum, penicillin (100 U/ml), streptomycin (100 µg/ml), glutamine (2 mM) and 1% non-essential amino acids. Cells were transfected using JetPRIME reagent and according to the manufacturer's protocol. Forty-eight hours after transfection, cells were washed with Dulbecco's phosphate buffered saline (PBS) and dissociated with 0.05% trypsin. Dissociated cells were collected after centrifugation at 1,000 rpm for 5 minutes at 4°C. The proteins were extracted from the collected pellets of HEK293T cells expressing either one of the four proteins (the protein that corresponds to full-length KIF1A/25B, the protein that corresponds to full-length KIF1A protein excluding exon 25B, the protein that corresponds to exon 25B alone and the protein that corresponds to EGFP) following two different procedures. When the protein samples were used for WB immunodetection uniquely, the cell pellets were re-suspended in 0.5% sodium dodecyl sulfate (SDS), 8M urea, 2% β-mercaptoethanol and protease inhibitor at 1X (cOmplete protease inhibitor cocktail, Sigma-Aldrich). This was followed by sonication of the pellets three times at 60 amplitudes and 4 seconds' pulse. The proteins were quantified using Bradford assay. When the protein samples were used for the co-IP, the collected pellets of the HEK293T cells were thawed on ice and re-suspended in co-IP lysis buffer. This buffer contains 50mM HEPES at pH=7.5, 10% glycerol, 150mM NaCl, 1.5mM ethylene glycol tetra-acetic acid (EGTA), 1% triton and protease inhibitor at 1X (cOmplete protease inhibitor cocktail, Sigma-Aldrich). This is followed by trituration of the cells 10 times by aspiration using a

20½ G needles, incubation on ice for 1 hour and centrifuge at 13,000 rpm for 15 minutes at 4°C. The supernatants were collected and the protein lysates were quantified by a Bradford assay.

2.1.1.3 Western blot (WB) immunodetection of recombinant proteins expressed in HEK293T cells

The proteins were denatured by adding SDS sample buffer (SSB) (50mM Tris-HCl at pH=6.8, 2% SDS, 10% glycerol, 1% β-mercaptoethanol, 0.02 % bromophenol blue) and SUB (0.5% SDS, 8M urea, 2% β-mercaptoethanol) to the proteins and leaving them in boiling water for 8 minutes. The ratio of protein lysates to denaturing buffers was about 1:3 depending on the protein lysates concentration; 5µl SSB is added to 20µg protein plus SUB for a total volume of 20µl. The proteins were fractionated by SDS-polyacrylamide gel electrophoresis (SDS-PAGE) and transferred to a polyvinylidene difluoride (PVDF) membrane using a transfer apparatus according to the manufacturer's protocol (Bio-Rad). The membrane was blocked in 5% milk, PBS and 0.2% tween overnight at 4°C.

Following the blockage, the membrane was incubated with monoclonal mouse anti-c-Myc antibody (2.1mg/mL, Sigma-Aldrich) for 1 hour at room temperature; this antibody was diluted 5,000 times in 5% milk, PBS and 0.2% tween. The membrane was washed 5 times in PBS and 0.2% tween; each wash lasted for 10 minutes. After the wash, the membrane was incubated with a horseradish peroxidase-conjugated donkey anti-mouse IgG (0.8mg/mL, Jackson ImmunoResearch) for 1 hour at room temperature; this

antibody was diluted 20,000 times in 5% milk, PBS and 0.2% tween. The membrane was washed with PBS and 0.2% tween five times (each wash lasted for 10 minutes) and developed with the ECL system (Bio-Rad) according to the manufacturer's protocols.

2.1.1.4 Immunoprecipitation and mass spectrometry analysis of KIF1A/25B

The co-IP was performed in two sets of triplicates simultaneously. Three mice were sacrificed and their spinal cords were dissected. To extract the proteins from the spinal cord, it was homogenized within 2mL SUB and protease inhibitor at 1X (cOmplete protease inhibitor cocktail, Sigma-Aldrich), using a Mastercraft drill and potter. The homogenized solution was sonicated six times at amplitude 60 for a 3 to 4 seconds' pulse. Following the sonication, the spinal cord extracts were centrifuged at 14,000 rpm for 30 minutes at 4°C. The supernatant proteins were quantified using Bradford assay.

50µl magnetic beads (Dynabeads protein G, Life Technology) were washed three times with cold PBS and 0.02% tween. 600µg proteins corresponding to each of the four constructs were pre-cleared (incubated with 50µl of magnetic beads for 1 hour at 4°C). The pre-cleared lysates were incubated overnight at 4°C with the magnetic beads pre-coupled and cross-linked to monoclonal mouse anti-c-Myc antibody (2.1mg/mL, Sigma-Aldrich). The samples were washed in cold PBS. 600µg of protein lysates extracted from spinal cord were also pre-cleared (incubated with 50µl of magnetic beads for 1 hour at 4°C). The pre-cleared spinal cord lysates were incubated with any of the four Myc tag bait constructs overnight at 4°C. The samples were washed in cold PBS and the remaining

proteins bound to the beads were used for mass spectrometry analysis in one set of the samples and used for confirming the presence of protein bands using stain free SDS-PAGE in another set of samples.

Mass spectrometry samples were analyzed using Mascot (Matrix Science, London, UK; version 2.4.1). Scaffold (version Scaffold_4.3.4, Proteome Software Inc., Portland, OR) was used to validate peptides and protein identifications. Peptides identifications were considered to be valid if they could be established to present a greater than 95.0 % probability by the Peptide Prophet algorithm[164].

2.1.1.5 Immunoprecipitation confirming the SYT11-KIF1A/25B interaction

The HEK293T cells were co-transfected with either full-length KIF1A/25B and SYT11, KIF1A minus exon 25B and SYT11 or EGFP and SYT11. 50µl magnetic beads (Dynabeads protein G, Life Technology) were washed three times with cold PBS and 0.02% tween. 300µg of proteins collected from HEK29T cells post co-transfection were pre-cleared (incubated with 50µl of magnetic beads for 1 hour at 4°C). The pre-cleared lysates were incubated for 1 hour at room temperature with the magnetic beads pre-coupled and cross-linked to monoclonal mouse anti-c-Myc antibody (2.1mg/mL, Sigma-Aldrich). Mouse IgG isotype control (0.5mg/mL, R&D Systems) was used for the co-IP as a negative control. The samples were washed in cold PBS and the remaining proteins bound to the beads were used for WB immunodetection (refer to section 2.1.1.3 for the procedure). The mouse monoclonal anti-Flag antibody (Sigma-Aldrich) was used to

detect SYT11. The protein extract from non-transfected cells was used as a negative control.

2.1.2 ESTABLISH THE EXPRESSION PROFILE OF KIF1A/25B IN WILD TYPE MICE

WB immunodetection was performed using tissues from adult wild-type C57BL/6J mice and a rabbit polyclonal antiserum developed in our laboratory in collaboration with Capralogics laboratory. The antiserum was raised against a specific peptide sequence of the murine orthologue region encoding the exon 25B. This sequence is positioned from amino acid 934 to 952 of KIF1A/25B protein, accession number: AB290172. The amino acid sequence of this peptide is LCDGRDPFYDRPPLFSLVG. The protein lysates are prepared from the nervous tissues (olfactory bulb, midbrain, hindbrain, cortex, cerebellum and spinal cord) and non-nervous tissues (kidney, liver, and lung). The expression profile in brain is partly validated through immunofluorescence (IF) assay on tissues of adult wild-type C57BL/6J animals.

2.1.2.1 Western Blot (WB) immunodetection of mouse tissues

To extract the proteins from the tissues, they were homogenized in different volumes (1 to 3 mL) of SUB containing protease inhibitor at 1X (cOmplete protease inhibitor, Sigma-Aldrich) using a Mastercraft drill with potters. The homogenized solution was sonicated six times at 60 amplitudes with a 3 to 4 seconds' pulse. Following the

sonication, the extracts were centrifuged at 14,000 rpm for 30 minutes at 4°C. The supernatant proteins were quantified using a Bradford assay.

20µg proteins were denatured (in SSB and SUB buffer boiled in a water bath for 8 minutes), fractionated by SDS-PAGE and transferred to a PVDF membrane using a transfer apparatus according to the manufacturer's protocol (Bio-Rad). The membrane was blocked in 5% milk, PBS and 0.2% tween overnight at 4°C. Following the blockage, the membrane was incubated with rabbit anti-KIF1A/25B antibody overnight at 4°C; the antibody was diluted 500 times in 5% milk, PBS and 0,2% tween. The membrane was washed 5 times in PBS and 0.2% tween; each wash lasted 10 minutes. After the wash, the membrane was incubated with a horseradish peroxidase-conjugated donkey anti-rabbit IgG (0.8 mg/mL, Jackson ImmunoResearch) for 1 hour at room temperature; this antibody was diluted 20,000 times in in 5% milk, PBS and 0,2% tween. The membrane was washed with PBS and 0.2% tween five times (each wash lasted 10 minutes) and developed with the ECL system (Bio-Rad) according to the manufacturer's protocols.

Peptide competition assay was performed to test the specificity of the anti-KIF1A/25B antibody. To do so, 2% antibody was incubated overnight at 4°C with the peptide against which the antibody was designed, 2% Normal Goat Serum (NGS) and PBS. In a control solution, no peptide was incubated with the antibody and in the other samples the antibody to peptide ratios was 1:200 and 1:500.

2.1.2.2 Immunofluorescence assay (IF) of mouse brain tissue

Cryosections of adult wild-type C57BL/6J mice brain tissue with the thickness of 20µm were prepared. The cryosections were washed with PBS and placed in citrate buffer at 85°C for an hour to retrieve the antigen. Afterward, they were washed three times with PBS and 0.02% triton (10 minutes' interval for each wash). The sections were blocked with 10% NGS, PBS and 0.02% triton. Then they were incubated with anti-KIF1A/25B antibody (the antibody was incubated overnight at 4°C with no peptide or with antibody to peptide ratios of 1:200 and 1:500 (refer to section 2.1.2.1 for detailed procedure).

The following day, the tissues were washed three times with PBS and incubated with secondary antibody for one hour at room temperature. Polyclonal donkey anti-rabbit IgG conjugated with Alexa Fluor® 488 (Invitrogen) was diluted 500 times in 2% NGS and PBS and was used as the secondary antibody. TOTO™-1 Iodide (Invitrogen) was used as a marker of the nucleus since it stains nucleic acids; it was diluted 300 times in PBS and 0.02% triton. Afterward the tissues were washed three time with PBS and mount with ProLong (Invitrogen). The tissues were dried overnight and the confocal microscopy was performed the day after.

2.2 Results

2.2.1 SCREEN FOR PROTEIN INTERACTORS OF KIF1A/25B

To identify the proteins that interact with exon 25B of KIF1A, co-IP was performed for four proteins: I) the protein that corresponds to full-length KIF1A/25B, II) the protein that corresponds to full-length KIF1A protein excluding exon 25B, III) the protein that corresponds to exon 25B alone and IV) the protein that corresponds to EGFP; this protein was used as a negative control. Using four different bait proteins helps to eliminate candidates that interact with all four amino acid sequences and allow priority to be given to interactors that are specific to exon 25B. Novel candidate interactors were detected using a LC-MS approach.

2.2.1.1 Western blot (WB) immunodetection of recombinant proteins expressed in HEK293T cells

Prior to performing the co-IP, WB was performed to ensure that the proteins are expressed in HEK293T cells. The cells were transfected with any one of the four cDNA constructs. The blots of both full-length KIF1A/25B and full-length KIF1A minus exon 25B showed the protein band at the right molecular weight (slightly less than 250 kDa). The protein extracts from non-transfected HEK293T cells were used as a negative control and no protein band was detected on the blot for this control (Figure 2.1).

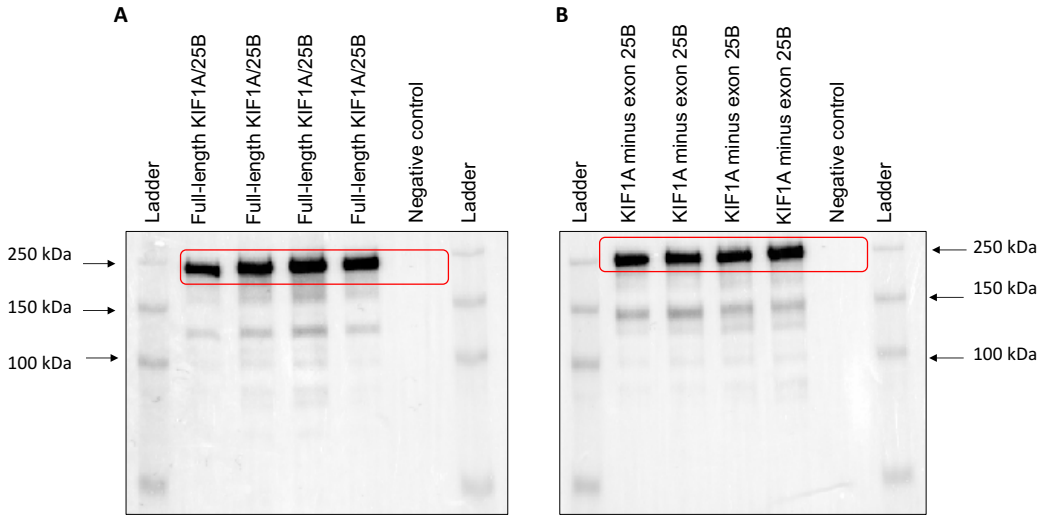

Figure 2.1: WB immunodetection of KIF1A/25B and KIF1A minus exon 25B

WB immunodetection of the protein extracts of HEK293T cells transfected with (A) full-length KIF1A/25B and (B) full-length KIF1A minus exon 25B PCS2 vector using anti-Myc antibody. The cell transfection was performed four times. The protein extracts from non-transfected HEK293T cells were used as a negative control.

The expected molecular weight for exon 25B is 22 kDa while the blot showed molecular weight of about 37 kDa. To address this issue, prior to loading the samples on SDS-PAGE, they were left longer in boiling water (10, 15 and 20 minutes) to ensure complete denaturation of the proteins. This approach did not improve the quality of the results; however, adding urea in the gel (Urea-PAGE) and heating samples at lower temperature (using PCR machine) was helpful to detect the right protein band size after long exposure time (30minutes) in addition to larger protein band size. The protein extracts from non-transfected HEK293T cells were used as a negative control and no protein band was detected on the blot for this control (Figure 2.2).

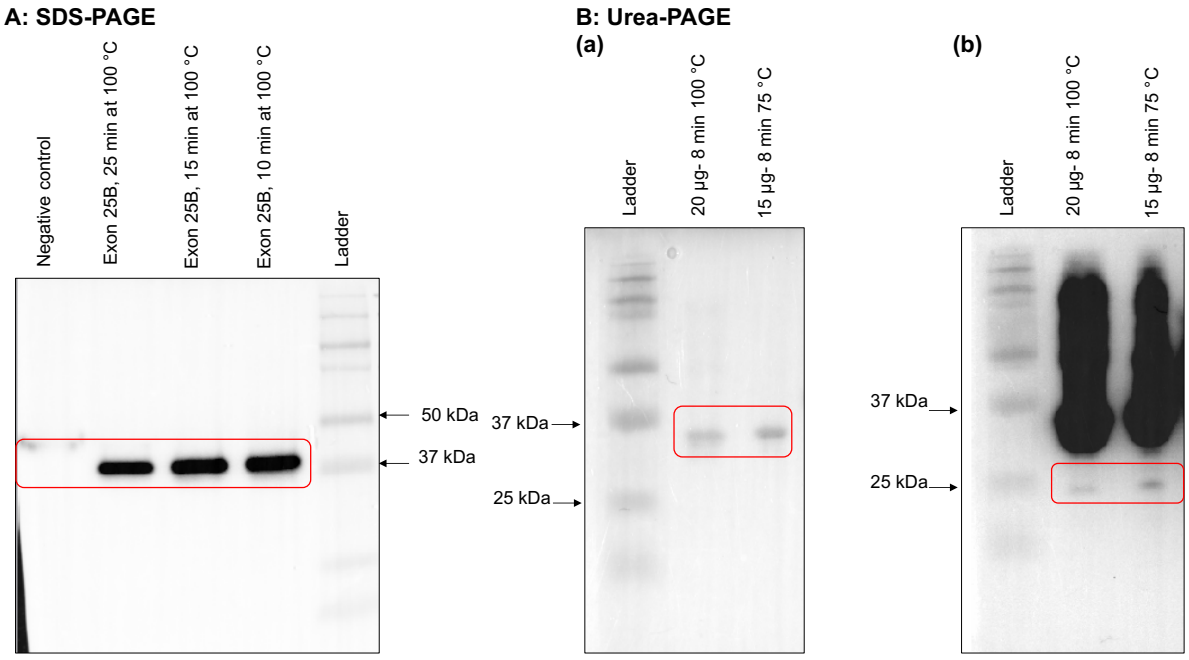

Figure 2.2: WB immunodetection of exon 25B

WB immunodetection of the protein extracts of HEK293T cells transfected with exon 25B PCS2 vector using anti-Myc antibody. (A) SDS-PAGE: the cell transfection was performed three times and the samples were left in boiling water for 10, 15 and 20 minutes. Protein extracts from non-transfected HEK293T cells were used as a negative control. (B) Urea-PAGE: the samples were heated either at 100°C or 75°C (a): low exposure (5 minutes), (b): long exposure (30 minutes).

For EGFP, the protein band with the right molecular weight (38 kDa) was detected. However, protein bands at 50 kDa and less than 37 kDa were also detected. To address this issue, prior to loading the samples on SDS-PAGE, they were left longer in boiling water (10, 15 and 20 minutes) to ensure complete denaturation of the proteins. Also, Urea-PAGE was used and the samples were heated at lower temperature (using PCR machine). Using Urea-PAGE and heating samples at 75°C improved the quality of the result slightly; a sharper EGFP protein band was observed. The protein extracts from non-

transfected HEK293T cells were used as a negative control and no protein band was detected on the blot for this control (Figure 2.3).

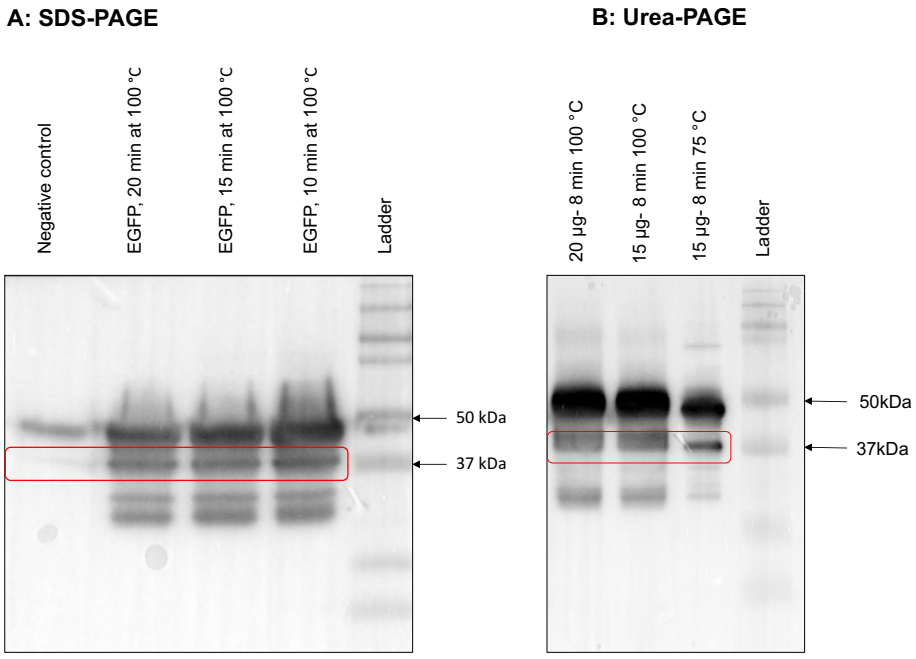

Figure 2.3: WB immunodetection of EGFP

WB immunodetection of the protein extracts of HEK293T cells transfected with EGFP PCS2 vector using anti-Myc antibody. (A) SDS-PAGE: the cell transfection was performed three times and the samples were left in boiling water for 10, 15 and 20 minutes. Protein extracts from non-transfected HEK293T cells were used as a negative control. (B) Urea-PAGE: the samples were heated either at 100°C or 75°C.

2.2.1.2 Immunoprecipitation and mass spectrometry analysis of KIF1A/25B

In order to perform the co-IP in triplicates, the spinal cord of three mice were dissected. To ensure that the dissection was performed properly and the spinal cord proteins were not denatured, the protein extracts were fractioned on a stain free SDS-PAGE and an image was taken. Sharp protein bands on the gel and the lack of smears on the gel confirmed that the proteins were not denatured (Figure 2.4).

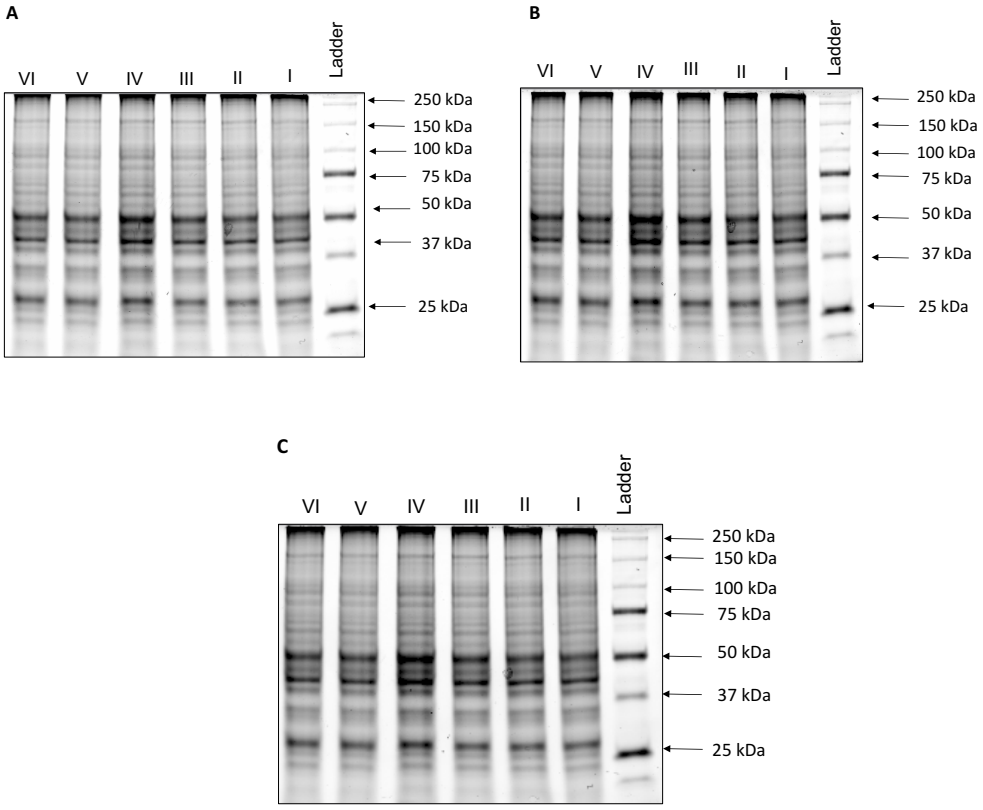

Figure 2.4: Stain free gel of mice spinal cord protein extracts

Stain free gel of the spinal cord protein extracts of three mice used in the co-IP. The samples were loaded six times (I-VI); mouse one (A), mouse two (B) and mouse three (C).

As indicated above, the co-IP was performed in two sets of triplicates using three mice spinal cord proteins. One set was tested by 7.5% stain free gel as a quality control. The immunoprecipitate (IP) of full-length KIF1A/25B and full-length KIF1A minus exon 25B showed a protein band with the molecular weight of about 200 kDa suggesting the presence of bait protein. The IP of both exon 25B and EGFP showed a protein band with molecular weight of about 30 kDa suggesting the presence of bait protein (Figure 2.5); if a 12% or 15% gel was used, a more accurate molecular weight would be observed. The same results were obtained for all three sets of experiments, mouse one to three.

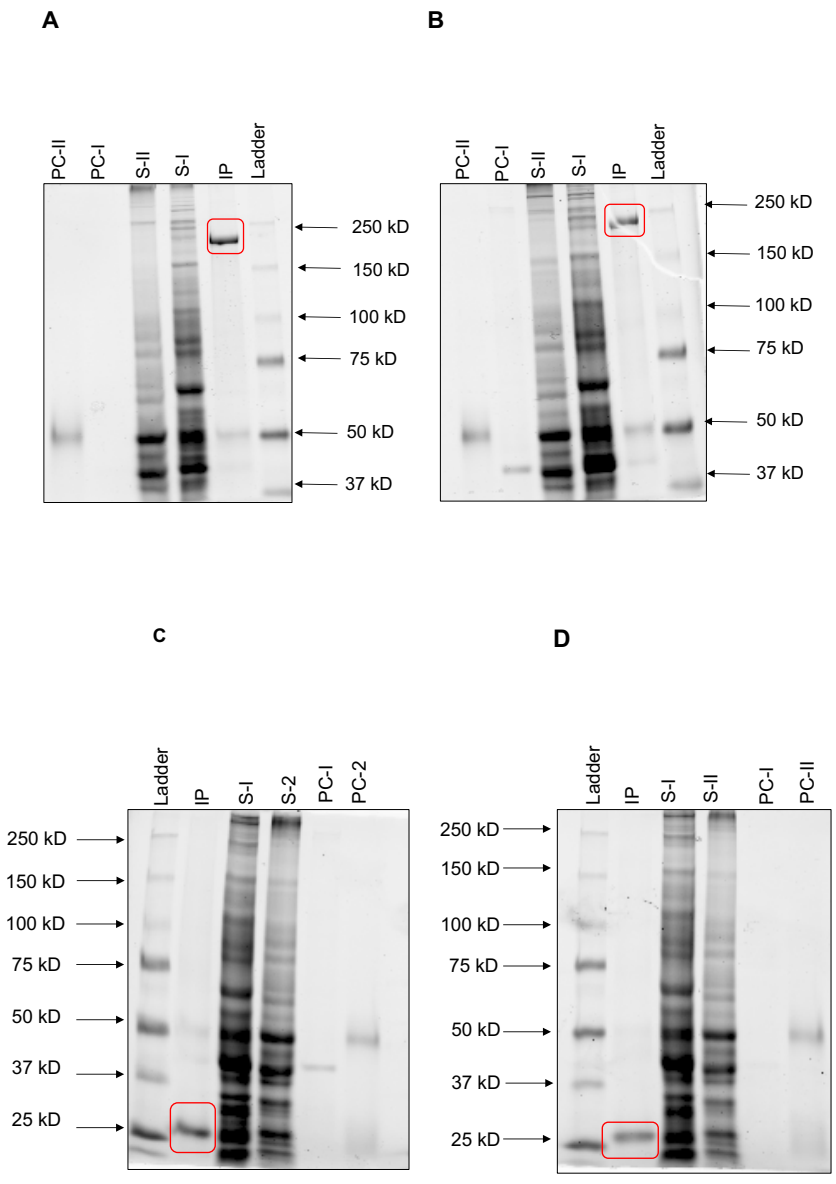

Figure 2.5: Stain free gel showing the co-IP of KIF1A/25B (A), KIF1A minus exon 25B (B), exon 25B (C) and EGFP (D) proteins

S: supernatant, PC: pre-cleared. S-I: HEK293T cell protein extracts ran over the beads. S-II: spinal cord protein extracts of mouse one ran over the beads. PC-I: beads pre-cleared with HEK293T cell protein extracts. PC-II: beads pre-cleared with spinal cord protein extracts of mouse one.

Since the co-IP was performed in triplicate, three lists of immunoprecipitated proteins were obtained from tandem mass spectrometry of each protein bait. These three sets of proteins were overlapped via Venn diagram. In full-length KIF1A/25, exon 25B and EGFP triplicates, more than 50% of the immunoprecipitated proteins were identical. In full-length KIF1A minus exon 25B, one set of samples had very low number of spectra; therefore, it was eliminated from the analyses.

Tandem mass spectrometry identified a total number of 545 co-immunoprecipitated proteins. The proteins that were identified in the EGFP samples and any of the other three protein baits (full-length KIF1A/25B, KIF1A minus exon 25B, and exon 25B alone) were considered as background, possibly interacting with the fused tag or with the anti-Myc antibody itself. Since the focus of this project was to define the function of exon 25B, the proteins present in both full-length KIF1A/25B and KIF1A minus exon 25B were also eliminated. Proteins present in exon 25B alone and absent in full-length KIF1A/25B were also eliminated since the exon 25B does not exist in nature. A total of 54 proteins were uniquely present in both full-length KIF1A/25 and exon 25B, but absent in full- length KIF1A minus 25B (Figure 2.6). Out of 54 possible interactors, 38 proteins were selected as possible true interactor based on their relevant function and location in neurons and synapses (Table S1).

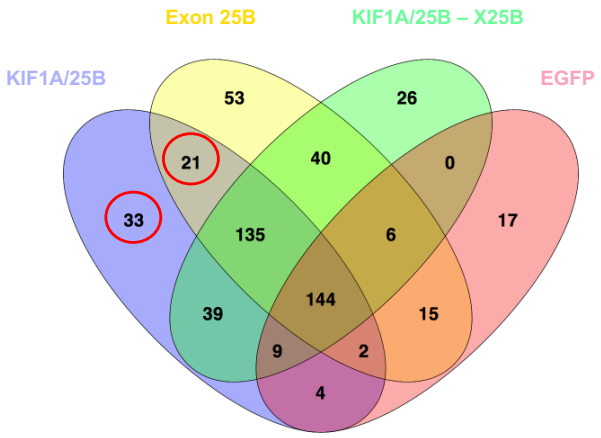

Figure 2.6: Venn diagram of the number of proteins identified by mass spectrometry

Red circles represents proteins that are considered as potential KIF1A/25B interactors. Purple oval: full-length KIF1A/25B co-immunoprecipitated proteins; green oval: full-length KIF1A minus exon 25B co-immunoprecipitated proteins; yellow oval: exon 25B immunoprecipitated proteins; pink oval: EGFP immunoprecipitated proteins.

2.2.1.2 Immunoprecipitation confirming KIF1A/25B-SYT11 interaction

One of the possible true interactors of KIF1A/25B is SYT11 (Table S.1); therefore, an attempt was made to confirm this interaction via co-IP. The protein extracts of HEK293T cells co-transfected with either full-length KIF1A/25B and SYT11, KIF1A minus exon 25B and SYT11 and EGFP and SYT11 were used to perform the co-IP. The protein extracts from non-transfected cells were used as a negative control. Full-length KIF1A/25B, KIF1A minus exon 25B and EGFP proteins were pulled down using anti-Myc antibody and their interaction with SYT11 was revealed by performing WB using mouse monoclonal anti-Flag antibody (Sigma-Aldrich). Mouse anti-IgG antibody was used for the

co-IP as a negative control. The WB of the negative control showed no protein band, as expected (Figure 2.7). Also, SYT11 protein band at molecular weight of about 60 kDa was not detected in IP of EGFP confirming the lack of interaction between EGFP and SYT11; however, the SYT11 protein band is detected in both full-length KIF1A/25B and KIF1A minus exon 25B (Figure 2.7).

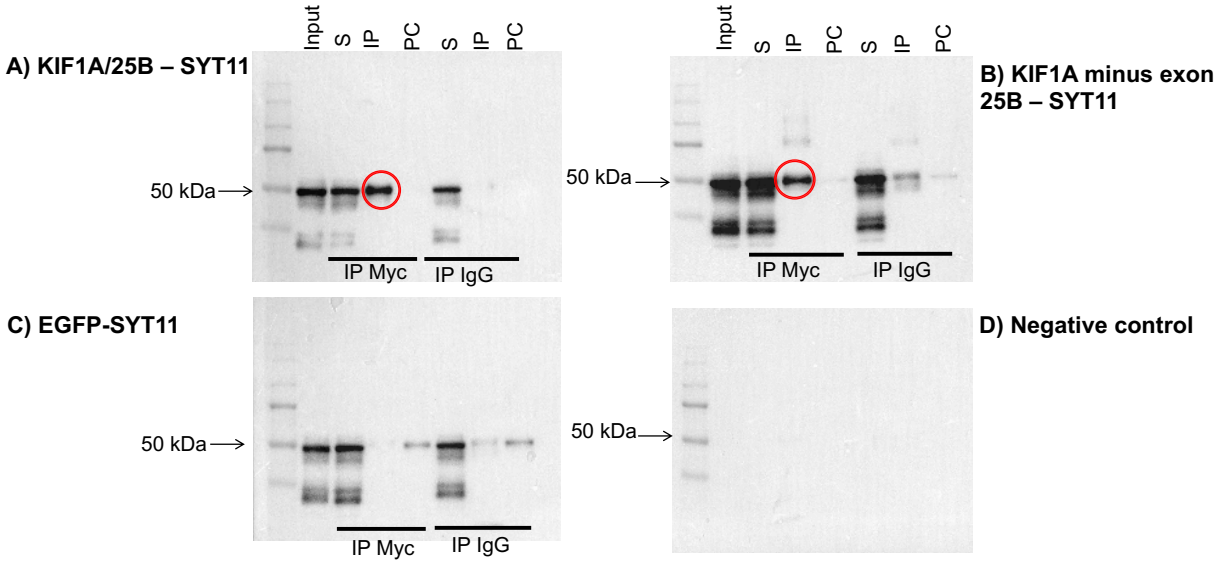

Figure 2.7: Co-IP of KIF1A/25B-Myc, KIF1A minus exon 25B-Myc and EGFP-Myc with SYT11-Flag

HEK293T cells were co-transfected with KIF1A/25B and SYT11 (A), KIF1A minus exon 25 and SYT11 (B), EGFP and SYT11 (C). Co-IP was performed using mouse anti-Myc antibody. Mouse anti-IgG antibody was used for the co-IP as a negative control. The eluted proteins were analysed by WB immunodetection using mouse anti-Flag antibody for the detection. IP: co-immunoprecipitated proteins after the elution. S: supernatent of the proteins that were incubated with the beads. PC: proteins eluted from the pre-clearing.

2.2.2 ESTABLISH THE EXPRESSION PROFILE OF KIF1A/25B IN WILD TYPE MICE

2.2.2.1 Western Blot (WB) immunodetection of mouse tissues

WB experiment were performed to verify the expression profile of KIF1A/25B. Detection of KIF1A/25B protein in olfactory bulb, cortex, midbrain, hindbrain, cerebellum and spinal cord protein lysates and the absence of detection in liver, lung and kidney protein lysates suggest that KIF1A/25B protein is highly present in nervous system and absent in non- nervous tissues (Figure 2.8).

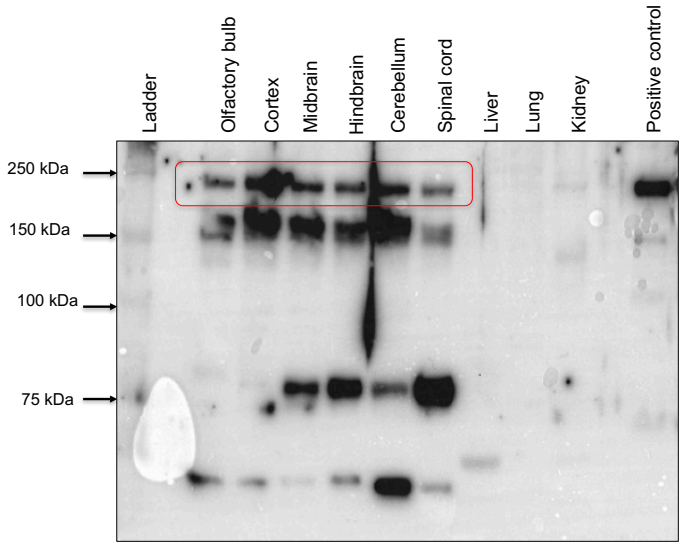

Figure 2.8: WB immunodetection of adult wild-type mice tissues

The WB immunodetection showing the expression profile of Kif1a/25b in protein lysates extracted from adult wild-type C57BL/6J mice. The protein extracts of HEK293T cells transfected with the full-length KIF1A/25B construct were used as a positive control.

The peptide competition assay was performed to test the specificity of the polyclonal rabbit anti-KIF1A/25B antibody (Figure 2.9). The protein extracts from different

tissues of adult wild type C57BL/6J mice were used. The protein extracts of HEK293T cells transfected with full-length KIF1A/25B construct were used as the positive control. The control blot showed the presence of KIF1A/25B protein in cortex and cerebellum and its absence in lung and liver. Considering the attenuation of signal observed in the 1:200 and 1:500 (antibody to peptide ratio) solutions compared to the control solution, the anti-KIF1A/25B antibody appears to be specific; however, detection of non-specific products in brain protein lysates bring the specificity of this antibody into question.

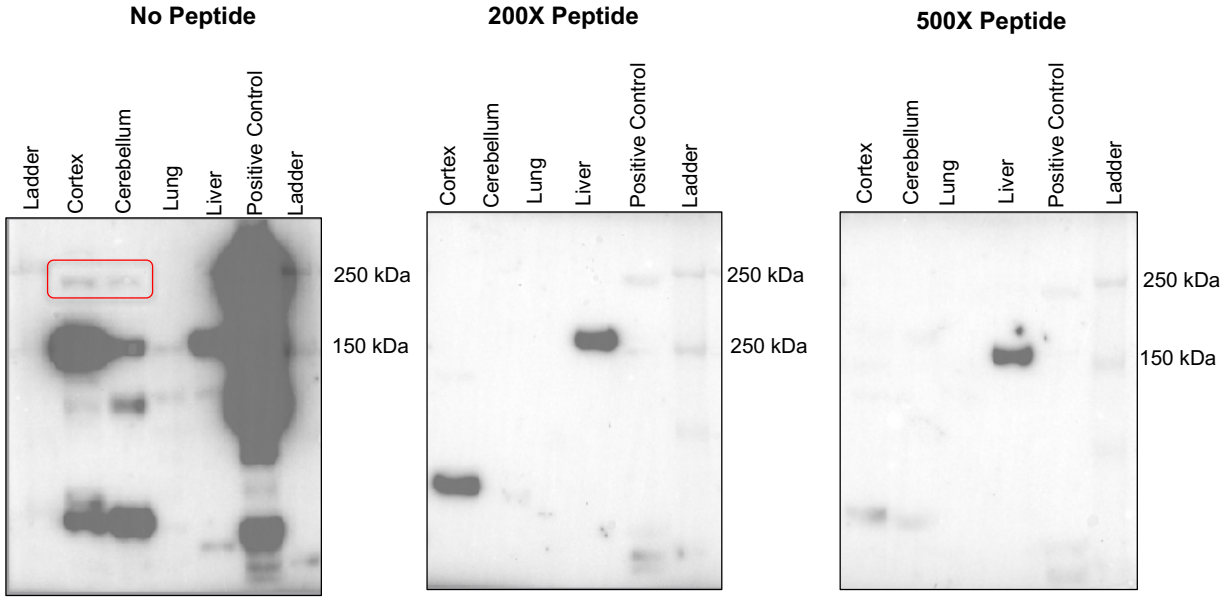

Figure 2.9: Peptide competition assay of adult wild type C57BL/6J mice protein extracts using anti-KIF1A/25B antibody

Protein lysates were prepared from adult wild-type C57BL/6J mice. Protein extracts of HEK293T cells transfected with the full-length KIF1A/25B construct were used as positive control. The peptide competition assay showed the attenuation of signal in 200X and 500X peptide compared to control (no peptide).

2.2.2.2 Immunofluorescence (IF) assay of mouse brain tissue

To verify the cellular localization of KIF1A/25B and to test the specificity of the polyclonal rabbit anti-KIF1A/25B antibody, IF experiment along with peptide competition assay was performed using cryosections of adult wild-type C57BL/6J mice (Figure 2.10). The confocal microscopic images validated the expression of KIF1A/25B protein in cerebellar tissue; specifically in Purkinje cells where it is highly expressed. The attenuation of signal observed in peptide competition assay suggested that the anti-KIF1A/25B antibody is indeed detecting the target protein; however, background signals suggested that this antibody lacks perfect specificity.

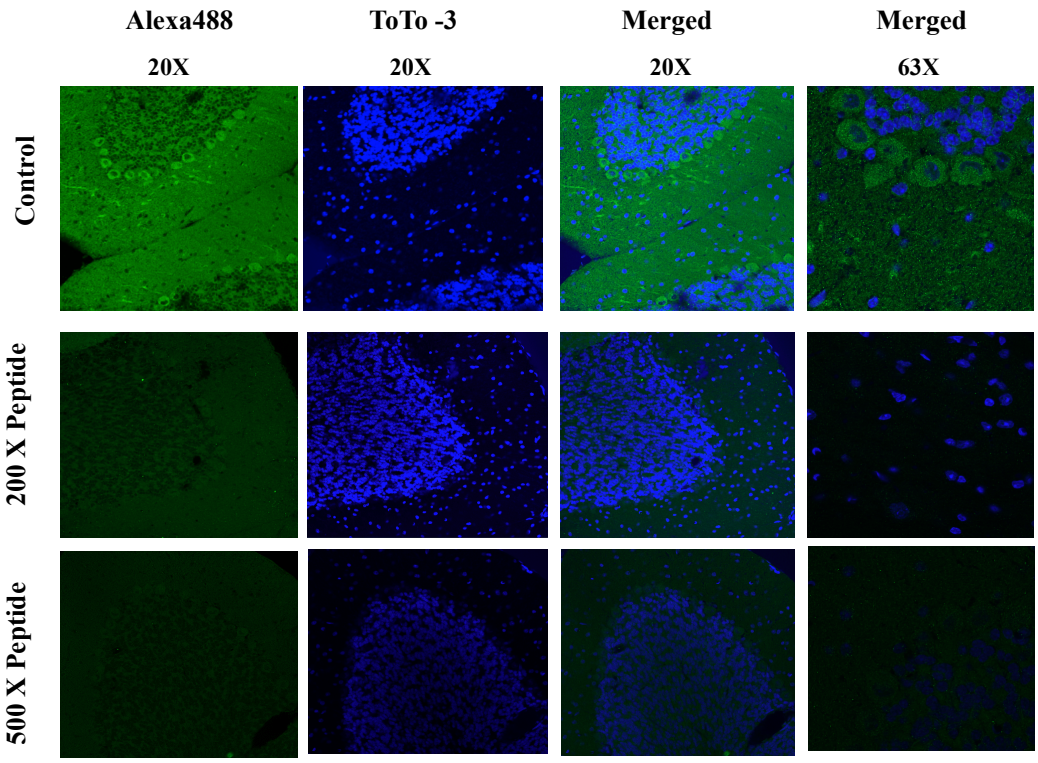

Figure 2.10: The confocal microscopic images of adult wild type C57BL/6J mice cerebellar tissue showing the localization of KIF1A/25B protein in Purkinje cells

The peptide competition assay showed the attenuation of signal in 200X and 500X peptide compared to control. For the immunofluorescence experiment, rabbit polyclonal anti-KIF1A/25B was used with donkey anti-rabbit IgG conjugated with Alexa Fluor® 488 (green) as the secondary antibody. TOTO™-1 Iodide was used as a nucleus marker. The images were taken at two magnifications (20X and 63X).

CHAPTER 3: DISCUSSION

3.1 GENERAL RESULTS

The major aim of this thesis was to understand the pathophysiology of HSAN-II. It has been reported that mutations in an alternatively spliced exon of *WNK1* gene are responsible for the development of HSAN-II (*WNK1/HSN2* isoform). Also, it has been reported that a specific isoform of *KIF1A* gene (*KIF1A/25B isoform*) is mutated in HSAN-II patients and this isoform interact with *WNK1/HSN2* isoform. In this study, we tried to understand how mutation in exon 25B of *KIF1A* gene (an axonal kinesin motor transporter) leads to HSAN-II. Defining the interacting partners of KIF1A/25B protein that are associated with cellular processes relevant to the HSAN-II pathology and defining the cellular localization of KIF1A/25B protein are major steps in characterizing the function of this protein.

3.1.1 SCREEN FOR PROTEIN INTERACTORS OF KIF1A/25B

Novel KIF1A/25B interacting partners were revealed by performing co-IP (using anti-Myc antibody) followed by mass spectrometry. Human KIF1A/25B cDNA was tagged in C-terminal with Myc tag and cloned in a pCS2 expression vector; this construct was used for the generation of exon 25B and KIF1A minus exon 25B construct using Gibson assembly[163]. EGFP tagged with Myc tag in C-terminal was used as a negative control. Using four different bait proteins helps to eliminate candidates that interact with all four proteins and allow priority to be given to interactors that are specific to exon 25B. Human

and mouse KIF1A protein share 91% identity; therefore, human cDNA is used as a bait protein (BLAST, https://blast.ncbi.nlm.nih.gov/Blast.cgi).

WB immunodetection of both full-length KIF1A/25B and KIF1A minus exon 25B showed the protein bands with the right molecular weight confirming the expression of these proteins in HEK293T cells (Figure 2.1).

WB immunodetection of exon 25B showed protein bands with a higher molecular weight than expected, 37 kDa instead of 22 kDa (Figure 2.2). When the protein samples were heated at 100°C longer (for up to 25 minutes), no change in the MW of the proteins was observed. However, when the protein samples were heated in SUB at lower temperature (75°C) and when urea was added to the gel, we were able to detect the right molecular weight at long exposure (30 minutes). This could be because at very high temperature, the breakdown of urea to cyanate ion is accelerated and the amino terminal of the exon 25B proteins form a chemical bond with the cyanate ion leading to carbamylation of the proteins[165]. It is known that the carbamoylated derivatives of the proteins have different retention time and mass compared to native protein[165]. Also, it is possible that the higher molecular weight protein band corresponds to exon 25B that is modified post-translationally.

WB immunodetection of EGFP showed an intense protein band at a higher molecular weight than what expected (about 50 kDa instead of 38.5 kDa) (Figure 2.3). It has been found that florescent proteins have the tendency to form oligomer[166,167]. Therefore, this protein band with a higher molecular weight could result from EGFP oligomerization or it could result from post-translational modifications of EGFP protein.

Same as the case of exon 25B, heating the protein samples at 100°C for longer (for up to 25 minutes) did not help in the process of the protein denaturation. However, heating EGFP proteins dissolved in SUB at lower temperature (75°C) and adding urea in the gel improved the quality of the result; this explains why heating urea at high temperature should be avoided.

The mass spectrometry results showed that the triplicates of full-length KIF1A/25B, exon 25B alone and EGFP and duplicate of KIF1A minus exon 25B share more than 50% of protein interactors. Moreover, KIF1A protein is one the 545 detected proteins in the mass spectrometry results, as expected. These findings suggest that the co-IP and mass spectrometry experiments were performed successfully.

As mentioned earlier, a yeast two-hybrid screen (Y2H) detected that KIF1A/25B isoform interact with WNK1/HSN2 isoform[156]; therefore, it was expected to have WNK1 protein as one of the KIF1A/25B interactors in the mass spectrometry results. However, we did not detect WNK1 protein neither in full-length KIF1A/25B nor in KIF1A minus exon 25B. It is possible that this protein is not highly expressed in mice spinal cord and the interaction is not abundant enough to be detected by mass spectrometry. It is also possible that WNK1/HSN2-KIF1A/25B interaction is a transient interaction or with a low affinity; therefore, it is not detectable by co-IP.

The Venn diagram showed that 54 proteins were uniquely present in both full-length KIF1A/25B and exon25B, but absent in KIF1A minus exon 25B and EGFP (Figure 2.6). We tried to confirm the interaction of one of these 54 proteins with KIF1A/25B via co-IP. We decided to focus on KIF1A/25B-SYT11 interaction because SYT11 is reported to be

involved in clathrin coated vesicle trafficking and neurotransmission[168].

Neurotransmission is the fundamental biological event that defines the neuronal communication and brain function[169]. In neurotransmission, when action potential arrives at axon terminal, the Ca^{2+} flows in axon terminal and trigger vesicle exocytosis. The neurotransmitters diffuse across the synaptic cleft and activate or inhibit the postsynaptic vesicle depending on their structure. After exocytosis, the synaptic vesicles are recycled via endocytosis; the endocytosis plays a crucial role for restoring synaptic vesicle and ongoing neurotransmission[170-172].

The endocytosis via clathrin-coated vesicles is the main pathway of synaptic vesicle protein internalization and plays a major role in recycling synaptic vesicles from the plasma membrane post exocytosis[172]. Syt11 is one of the proteins that is involved in balancing endocytosis and exocytosis[169]; it inhibits clathrin-mediated endocytosis and interferes with balanced endo-exocytosis and prevents the ongoing neurotransmission[168].

Synaptotagmins are a family of type I membrane-trafficking proteins either in synaptic vesicles or cellular membranes and so far, 17 mammalian Synaptotagmins isoforms have been identified[169]. Their molecular structure is defined by a N-terminal transmembrane domain, a linker and two highly conserved C-terminal tandem C_2 domains (C_2A and C_2B)[173]. The C_2 domains have two or three Ca^{2+} binding sites that mediates exocytosis. Most Synaptotagmins have the evolutionary conserved C_2 domains; however, SYT11 is not a calcium sensor and do not bind Ca^{2+} because of a substitution of aspartate for serine in a Ca^{2+} coordination site in C_2 domain[169,174]. The endocytosis

inhibitory role of SYT11 could explain why it lost its Ca^{2+} sensing function through the evolution[174].

The co-IP experiment (Figure 2.7) showed no SYT11 detection in protein extracts of non-transfected cells (negative also). Also, SYT11 was not immunoprecipitated with EGFP protein; this was expected based on mass spectrometry results. The mass spectrometry results showed SYT11 as a novel interactor of KIF1A/25B and not KIF1A minus exon 25B; however, the co-IP (Figure 2.7) showed that SYT11 interact with both KIF1A/25B and KIF1A minus exon 25B. This could be due to conformational change of SYT11 protein in mouse spinal cord versus those expressed in HEK293T cells. Also, the Flag tag in C-terminal of SYT11 could be the cause of this particular interaction in the co-IP setting. The interaction of SYT11 with KIF1A/25B and KIF1A minus exon 25B do not exist when IgG isotype control is used suggesting that this interaction is not a false positive result.

It would be interesting to pull down the KIF1A/25B and KIF1A minus exon 25B proteins with the anti-Myc antibody coupled and cross-linked to beads and run over the beads the mouse spinal cord protein extracts and detect the blot using mouse anti-SYT11 antibody. If the WB immunodetection shows no KIF1A minus exon 25B-SYT11 interaction, we could conclude that the interaction detected in figure 2.7 is due to conformational change of SYT11 expressed in HEK293T cells or the effect of Flag tag.

Another way of confirming KIF1A/25B-SYT11 interaction is to pull down SYT11 using anti-FLAG antibody coupled and cross-linked to beads and pass over the beads

the mouse spinal cord protein extracts. In this setting a specific mouse anti-KIF1A/25B antibody is required to detect the interaction.

Regarding KIF1A/25B-SYT11 interaction, It is interesting to know how this interaction affect the biological processes involved in the development of HSAN-II. In an experiment, KIF1A25B could be knockdown and the changes in localization of SYT11 and vesicle trafficking could be observed.

Another protein required for clathrin mediated endocytosis (CME) is clathrin coat assembly protein AP180 (gene name: snap91: synaptosome associated protein 91)[175](Table S1). Interestingly, this protein was found as one of the novel interactors of KIF1A/25B in our mass spectrometry results (Table S1). It has been reported that AP180 is required for recycling of synaptic vesicles and balanced inhibitory and excitatory neurotransmission[170]. AP180 could be one of the KIF1A/25B cargos and possibly the mutated KIF1A/25B is unable to transport AP180 protein from endoplasmic reticulum (ER), where the protein is made, towards where the endocytosis occurs and interfere with neurotransmission.

3.1.2 ESTABLISH THE EXPRESSION PROFILE OF KIF1A/25B IN WILD TYPE MICE

As HSAN-II is a neurological disorder and KIF1A/25B isoform is known to be the cause of this disorder, it is expected that this isoform be expressed in nervous tissues. WB immunodetection and immunofluorescence results confirmed the expression of KIF1A/25B isoform in the nervous tissues (olfactory bulb, cortex, midbrain, hindbrain,

cerebellum and spinal cord) and the lack of its expression in non-nervous tissues (lung, liver and kidney). Both WB immunodetection and immunofluorescence results showed certain degree of specificity for the rabbit anti-KIF1A/25B antibody. However, in the WB extra protein bands are noted at sizes smaller than target protein (KIF1A/25B). These protein bands might correspond to degradation products of the target protein or to proteins other than the KIF1A/25B protein.

The result of immunofluorescence assay could be improved should a new antibody that is more specific for the target protein is developed and thus produce images with a superior signal to noise ratio. In case the background is the result of auto-fluorescence, this component of the net signal can be quenched before performing this assay. Comparing our current immunofluorescence results with assays using other (non-cerebellar) nervous tissues would also provide a more complete understanding of the expression profile of KIF1A/25B.

3.2 GENERAL CONCLUSION

This study was conducted to expand our knowledge on the molecular pathogenesis of the HSAN-II pathology and the involvement of KIF1A/25B in the development of this disorder. Our results showed a likely interaction between KIF1A/25B and SYT11. Since KIF1A/25B is a kinesin motor that transport vesicles and cargos along the axon and since SYT11 plays a role in inhibiting clathrin-mediated endocytosis and balancing endo-exocytosis, KIF1A/25B-SYT11 interaction suggests that SYT11 could be one of the

KIF1A/25B cargos and mutation in KIF1A/25B eliminates KIF1A/25B-SYT11 interaction and inhibit balanced endocytosis-exocytosis and ongoing neurotransmission. Our work also showed interaction of KIF1A/25B with other proteins known to be implicated in endocytosis. Therefore, malfunctioning endocytosis could be one of the disease mechanisms of HSAN-II.

REFERENCES

1. Rinaldi, R. & Patel, A. Inherited polyneuropathies. *PM R* **5**, S63-73 (2013).

2. Shekarabi, M. *et al.* Mutations in the nervous system--specific HSN2 exon of WNK1 cause hereditary sensory neuropathy type II. *J Clin Invest* **118**, 2496-505 (2008).

3. Skre, H. Genetic and clinical aspects of Charcot-Marie-Tooth's disease. *Clin Genet* **6**, 98-118 (1974).

4. Merner, N., Dion, P., Szuto, A. & Rouleau, G. Insensitivity to pain: Lessons from recent genetics advances. in *Culture, Brain & Analgesia* (ed. Todd, M.I.a.K.H.) 317-333 (Oxford University Press, USA, 2013).

5. Dearborn, G. A case of congenital general pure analgesia. *J Nerv Ment Dis* **75**, 612-615 (1932).

6. Ford, F.R. & Wilkins, L. Congenital universal insensitiveness to pain. . *Bull John Hopkins Hosp* **62**, 448-466 (1938).

7. Boyd, D.A., Jr. & Nie, L.W. Congenital universal indifference to pain. *Arch Neurol Psychiatry* **61**, 402-12 (1949).

8. Winkelmann, R.K., Lambert, E.H. & Hayles, A.B. Congenital absence of pain. Report of a case and experimental studies. *Arch Dermatol* **85**, 325-39 (1962).

9. Jewesbury, E.C.O. (ed.) *Congenital indifference to pain.*, 187-204 (Elsevier, Amsterdam, 1970).

10. Dyck, P.J. *et al.* Not 'indifference to pain' but varieties of hereditary sensory and autonomic neuropathy. *Brain* **106 (Pt 2)**, 373-90 (1983).

11. Klein, C.J., Sinnreich, M. & Dyck, P.J. Indifference rather than insensitivity to pain. *Ann Neurol* **53**, 417-8; author reply 418-9 (2003).

12. Landrieu, P., Said, G. & Allaire, C. Dominantly transmitted congenital indifference to pain. *Ann Neurol* **27**, 574-8 (1990).

13. Nagasako, E.M., Oaklander, A.L. & Dworkin, R.H. Congenital insensitivity to pain: an update. *Pain* **101**, 213-9 (2003).

14. Goldberg, Y.P. *et al.* Loss-of-function mutations in the Nav1.7 gene underlie congenital indifference to pain in multiple human populations. *Clin Genet* **71**, 311-9 (2007).

15. Baxter, D.W. & Olszewski, J. Congenital universal insensitivity to pain. *Brain* **83**, 381-93 (1960).

16. Ervin, F.R. & Sternbach, R.A. Hereditary insensitivity to pain. *Trans Am Neurol Assoc* **85**, 70-4 (1960).

17. Comings, D.E. & Amromin, G.D. Autosomal dominant insensitivity to pain with hyperplastic myelinopathy and autosomal dominant indifference to pain. *Neurology* **24**, 838-48 (1974).

18. Dyck, P.J. Peripheral neuropathy. Changing concepts, differential diagnosis and classification. *Med Clin North Am* **52**, 895-908 (1968).

19. Hilz, M.J. Assessment and evaluation of hereditary sensory and autonomic neuropathies with autonomic and neurophysiological examinations. *Clin Auton Res* **12 Suppl 1**, I33-43 (2002).

20. Auer-Grumbach, M. Hereditary sensory and autonomic neuropathies. *Handb Clin Neurol* **115**, 893-906 (2013).

21. Mroczek, M., Kabzinska, D. & Kochanski, A. Molecular pathogenesis, experimental therapy and genetic counseling in hereditary sensory neuropathies. *Acta Neurobiol Exp (Wars)* **75**, 126-43 (2015).

22. Auer-Grumbach, M. *et al.* Autosomal dominant inherited neuropathies with prominent sensory loss and mutilations: a review. *Arch Neurol* **60**, 329-34 (2003).

23. Auer-Grumbach, M., Mauko, B., Auer-Grumbach, P. & Pieber, T.R. Molecular genetics of hereditary sensory neuropathies. *Neuromolecular Med* **8**, 147-58 (2006).

24. Verpoorten, N., De Jonghe, P. & Timmerman, V. Disease mechanisms in hereditary sensory and autonomic neuropathies. *Neurobiol Dis* **21**, 247-55 (2006).

25. Axelrod, F.B. & Gold-von Simson, G. Hereditary sensory and autonomic neuropathies: types II, III, and IV. *Orphanet J Rare Dis* **2**, 39 (2007).

26. Auer-Grumbach, M. Hereditary sensory neuropathy type I. *Orphanet J Rare Dis* **3**, 7 (2008).

27. Davidson, G. *et al.* Frequency of mutations in the genes associated with hereditary sensory and autonomic neuropathy in a UK cohort. *J Neurol* **259**, 1673-85 (2012).

28. Rotthier, A. *et al.* Genes for hereditary sensory and autonomic neuropathies: a genotype-phenotype correlation. *Brain* **132**, 2699-711 (2009).

29. Aguzzi, A. & Calella, A.M. Prions: protein aggregation and infectious diseases. *Physiol Rev* **89**, 1105-52 (2009).

30. Weis, J. *et al.* Towards a functional pathology of hereditary neuropathies. *Acta Neuropathol* **133**, 493-515 (2017).

31. Rotthier, A., Baets, J., Timmerman, V. & Janssens, K. Mechanisms of disease in hereditary sensory and autonomic neuropathies. *Nat Rev Neurol* **8**, 73-85 (2012).

32. Westergard, L., Christensen, H.M. & Harris, D.A. The cellular prion protein (PrP(C)): its physiological function and role in disease. *Biochim Biophys Acta* **1772**, 629-44 (2007).

33. Nicholson, G.A. *et al.* The gene for hereditary sensory neuropathy type I (HSN-I) maps to chromosome 9q22.1-q22.3. *Nat Genet* **13**, 101-4 (1996).

34. Dawkins, J.L., Hulme, D.J., Brahmbhatt, S.B., Auer-Grumbach, M. & Nicholson, G.A. Mutations in SPTLC1, encoding serine palmitoyltransferase, long chain base subunit-1, cause hereditary sensory neuropathy type I. *Nat Genet* **27**, 309-12 (2001).

35. Bejaoui, K. *et al.* SPTLC1 is mutated in hereditary sensory neuropathy, type 1. *Nat Genet* **27**, 261-2 (2001).

36. Rotthier, A. *et al.* Mutations in the SPTLC2 subunit of serine palmitoyltransferase cause hereditary sensory and autonomic neuropathy type I. *Am J Hum Genet* **87**, 513-22 (2010).

37. Rotthier, A. *et al.* Characterization of two mutations in the SPTLC1 subunit of serine palmitoyltransferase associated with hereditary sensory and autonomic neuropathy type I. *Hum Mutat* **32**, E2211-25 (2011).

38. Auer-Grumbach, M. *et al.* Mutations at Ser331 in the HSN type I gene SPTLC1 are associated with a distinct syndromic phenotype. *Eur J Med Genet* **56**, 266-9 (2013).

39. Hornemann, T. *et al.* The SPTLC3 subunit of serine palmitoyltransferase generates short chain sphingoid bases. *J Biol Chem* **284**, 26322-30 (2009).

40. Dawkins, J.L. *et al.* Exclusion of serine palmitoyltransferase long chain base subunit 2 (SPTLC2) as a common cause for hereditary sensory neuropathy. *Neuromuscul Disord* **12**, 656-8 (2002).

41. Gable, K. *et al.* Mutations in the yeast LCB1 and LCB2 genes, including those corresponding to the hereditary sensory neuropathy type I mutations, dominantly inactivate serine palmitoyltransferase. *J Biol Chem* **277**, 10194-200 (2002).

42. Hanada, K. Serine palmitoyltransferase, a key enzyme of sphingolipid metabolism. *Biochim Biophys Acta* **1632**, 16-30 (2003).

43. Merrill, A.H., Jr. Sphingolipid and glycosphingolipid metabolic pathways in the era of sphingolipidomics. *Chem Rev* **111**, 6387-422 (2011).

44. Penno, A. *et al.* Hereditary sensory neuropathy type 1 is caused by the accumulation of two neurotoxic sphingolipids. *J Biol Chem* **285**, 11178-87 (2010).

45. Fischer, D. *et al.* A novel missense mutation confirms ATL3 as a gene for hereditary sensory neuropathy type 1. *Brain* **137**, e286 (2014).

46. Kornak, U. *et al.* Sensory neuropathy with bone destruction due to a mutation in the membrane-shaping atlastin GTPase 3. *Brain* **137**, 683-92 (2014).

47. Hu, J. *et al.* A class of dynamin-like GTPases involved in the generation of the tubular ER network. *Cell* **138**, 549-61 (2009).

48. Chen, S., Novick, P. & Ferro-Novick, S. ER structure and function. *Curr Opin Cell Biol* **25**, 428-33 (2013).

49. Rismanchi, N., Soderblom, C., Stadler, J., Zhu, P.P. & Blackstone, C. Atlastin GTPases are required for Golgi apparatus and ER morphogenesis. *Hum Mol Genet* **17**, 1591-604 (2008).

50. Guelly, C. *et al.* Targeted high-throughput sequencing identifies mutations in atlastin-1 as a cause of hereditary sensory neuropathy type I. *Am J Hum Genet* **88**, 99-105 (2011).

51. Klein, C.J. *et al.* Mutations in DNMT1 cause hereditary sensory neuropathy with dementia and hearing loss. *Nat Genet* **43**, 595-600 (2011).

52. Feng, J. & Fan, G. The role of DNA methylation in the central nervous system and neuropsychiatric disorders. *Int Rev Neurobiol* **89**, 67-84 (2009).

53. Qin, W., Leonhardt, H. & Pichler, G. Regulation of DNA methyltransferase 1 by interactions and modifications. *Nucleus* **2**, 392-402 (2011).

54. Fox, R., Ealing, J., Murphy, H., Gow, D.P. & Gosal, D. A novel DNMT1 mutation associated with early onset hereditary sensory and autonomic neuropathy, cataplexy, cerebellar atrophy, scleroderma, endocrinopathy, and common variable immune deficiency. *J Peripher Nerv Syst* **21**, 150-3 (2016).

55. Smets, M. *et al.* DNMT1 mutations found in HSANIE patients affect interaction with UHRF1 and neuronal differentiation. *Hum Mol Genet* **26**, 1522-1534 (2017).

56. Bird, A. DNA methylation patterns and epigenetic memory. *Genes Dev* **16**, 6-21 (2002).

57. Goll, M.G. & Bestor, T.H. Eukaryotic cytosine methyltransferases. *Annu Rev Biochem* **74**, 481-514 (2005).

58. Cheng, X. & Blumenthal, R.M. Mammalian DNA methyltransferases: a structural perspective. *Structure* **16**, 341-50 (2008).

59. Law, J.A. & Jacobsen, S.E. Establishing, maintaining and modifying DNA methylation patterns in plants and animals. *Nat Rev Genet* **11**, 204-20 (2010).

60. Smith, Z.D. & Meissner, A. DNA methylation: roles in mammalian development. *Nat Rev Genet* **14**, 204-20 (2013).

61. Herrup, K. & Yang, Y. Cell cycle regulation in the postmitotic neuron: oxymoron or new biology? *Nat Rev Neurosci* **8**, 368-78 (2007).

62. Brooks, P.J., Marietta, C. & Goldman, D. DNA mismatch repair and DNA methylation in adult brain neurons. *J Neurosci* **16**, 939-45 (1996).

63. Fan, G. *et al.* DNA hypomethylation perturbs the function and survival of CNS neurons in postnatal animals. *J Neurosci* **21**, 788-97 (2001).

64. Wright, A. & Dyck, P.J. Hereditary sensory neuropathy with sensorineural deafness and early-onset dementia. *Neurology* **45**, 560-2 (1995).

65. Hojo, K. *et al.* Hereditary sensory neuropathy with deafness and dementia: a clinical and neuroimaging study. *Eur J Neurol* **6**, 357-61 (1999).

66. Kok, C. *et al.* A locus for hereditary sensory neuropathy with cough and gastroesophageal reflux on chromosome 3p22-p24. *Am J Hum Genet* **73**, 632-7 (2003).

67. Spring, P.J. *et al.* Autosomal dominant hereditary sensory neuropathy with chronic cough and gastro-oesophageal reflux: clinical features in two families linked to chromosome 3p22-p24. *Brain* **128**, 2797-810 (2005).

68. Murray, T.J. Congenital sensory neuropathy. *Brain* **96**, 387-94 (1973).

69. Ogryzlo, M.A. A familial peripheral neuropathy of unknown etiology resembling Morvan's disease. *Can Med Assoc J* **54**, 547-53 (1946).

70. Ota, M., Ellefson, R.D., Lambert, E.H. & Dyck, P.J. Hereditary sensory neuropathy, type II. Clinical, electrophysiologic, histologic, and biochemical studies of a Quebec kinship. *Arch Neurol* **29**, 23-37 (1973).

71. Kondo, K. & Horikawa, Y. Genetic heterogeneity of hereditary sensory neuropathy. *Arch Neurol* **30**, 336-7 (1974).

72. Ferriere, G., Guzzetta, F., Kulakowski, S. & Evrard, P. Nonprogressive type II hereditary sensory autonomic neuropathy: a homogeneous clinicopathologic entity. *J Child Neurol* **7**, 364-70 (1992).

73. Tamari, I. *et al.* Autosomal recessive peripheral sensory neuropathy in 3 non-Ashkenazi Jewish families. *J Med Genet* **17**, 424-9 (1980).

74. Lafreniere, R.G. *et al.* Identification of a novel gene (HSN2) causing hereditary sensory and autonomic neuropathy type II through the Study of Canadian Genetic Isolates. *Am J Hum Genet* **74**, 1064-73 (2004).

75. Kurth, I. *et al.* Mutations in FAM134B, encoding a newly identified Golgi protein, cause severe sensory and autonomic neuropathy. *Nat Genet* **41**, 1179-81 (2009).

76. Dyck, P.J. Neuronal atrophy and degeneration predominantly affecting peripheral sensory and autonomic neurons. in *Peripheral Neuropathy*, Vol. II (eds. Dyck, P.J., Thomas, P.K., Griffin, J.W., Low, P.A. & Podulso, J.F.) 1065-1093 (WB Saunders, Philadelphia, 1993).

77. Barry, J.E., Hopkins, I.J. & Neal, B.W. Congenital sensory neuropathy. *Arch Dis Child* **49**, 128-32 (1974).

78. Klebanoff, M.A. & Neff, J.M. Familial dysautonomia associated with recurrent osteomyelitis in a non-Jewish girl. *J Pediatr* **96**, 75-7 (1980).

79. Silveira, A.L., Binkowski, R.T., Rich, B.F., Benetti, M.B. & Almeida, A.M. Hereditary sensory and autonomic neuropathy type 3 in non-Jewish child. *Arq Neuropsiquiatr* **70**, 900-1 (2012).

80. Blumenfeld, A. *et al.* Localization of the gene for familial dysautonomia on chromosome 9 and definition of DNA markers for genetic diagnosis. *Nat Genet* **4**, 160-4 (1993).

81. Anderson, S.L. *et al.* Familial dysautonomia is caused by mutations of the IKAP gene. *Am J Hum Genet* **68**, 753-8 (2001).

82. Slaugenhaupt, S.A. *et al.* Tissue-specific expression of a splicing mutation in the IKBKAP gene causes familial dysautonomia. *Am J Hum Genet* **68**, 598-605 (2001).

83. Axelrod, F.B. Familial dysautonomia. *Muscle Nerve* **29**, 352-63 (2004).

84. Leyne, M. *et al.* Identification of the first non-Jewish mutation in familial Dysautonomia. *Am J Med Genet A* **118A**, 305-8 (2003).

85. Naumanen, T., Johansen, L.D., Coffey, E.T. & Kallunki, T. Loss-of-function of IKAP/ELP1: could neuronal migration defect underlie familial dysautonomia? *Cell Adh Migr* **2**, 236-9 (2008).

86. Hunnicutt, B.J., Chaverra, M., George, L. & Lefcort, F. IKAP/Elp1 is required in vivo for neurogenesis and neuronal survival, but not for neural crest migration. *PLoS One* **7**, e32050 (2012).

87. Hawkes, N.A. *et al.* Purification and characterization of the human elongator complex. *J Biol Chem* **277**, 3047-52 (2002).

88. Dietrich, P., Yue, J., E, S. & Dragatsis, I. Deletion of exon 20 of the Familial Dysautonomia gene Ikbkap in mice causes developmental delay, cardiovascular defects, and early embryonic lethality. *PLoS One* **6**, e27015 (2011).

89. Dietrich, P., Alli, S., Shanmugasundaram, R. & Dragatsis, I. IKAP expression levels modulate disease severity in a mouse model of familial dysautonomia. *Hum Mol Genet* **21**, 5078-90 (2012).

90. Indo, Y. *et al.* Mutations in the TRKA/NGF receptor gene in patients with congenital insensitivity to pain with anhidrosis. *Nat Genet* **13**, 485-8 (1996).

91. Altassan, R. *et al.* Exome sequencing identifies novel NTRK1 mutations in patients with HSAN-IV phenotype. *Am J Med Genet A* **173**, 1009-1016 (2017).

92. Schulman, H. *et al.* Congenital insensitivity to pain with anhidrosis (CIPA): the spectrum of radiological findings. *Pediatr Radiol* **31**, 701-5 (2001).

93. Kayani, B. *et al.* Orthopaedic manifestations of congenital indifference to pain with anhidrosis (Hereditary Sensory and Autonomic Neuropathy type IV). *Eur J Paediatr Neurol* **21**, 318-326 (2017).

94. Uehara, K. *et al.* Ankle arthrodesis and tibial lengthening for congenital sensory neuropathy with anhidrosis. *J Orthop Sci* **6**, 430-4 (2001).

95. Indo, Y. Neurobiology of pain, interoception and emotional response: lessons from nerve growth factor-dependent neurons. *Eur J Neurosci* **39**, 375-91 (2014).

96. Indo, Y. Molecular basis of congenital insensitivity to pain with anhidrosis (CIPA): mutations and polymorphisms in TRKA (NTRK1) gene encoding the receptor tyrosine kinase for nerve growth factor. *Hum Mutat* **18**, 462-71 (2001).

97. Nam, T.S. *et al.* Novel NTRK1 mutations associated with congenital insensitivity to pain with anhidrosis verified by functional studies. *J Peripher Nerv Syst* (2017).

98. Greco, A., Villa, R. & Pierotti, M.A. Genomic organization of the human NTRK1 gene. *Oncogene* **13**, 2463-6 (1996).

99. Kaplan, D.R. & Miller, F.D. Neurotrophin signal transduction in the nervous system. *Curr Opin Neurobiol* **10**, 381-91 (2000).

100. Wiesmann, C., Ultsch, M.H., Bass, S.H. & de Vos, A.M. Crystal structure of nerve growth factor in complex with the ligand-binding domain of the TrkA receptor. *Nature* **401**, 184-8 (1999).

101. Indo, Y. Nerve growth factor, pain, itch and inflammation: lessons from congenital insensitivity to pain with anhidrosis. *Expert Rev Neurother* **10**, 1707-24 (2010).

102. Indo, Y. Nerve growth factor and the physiology of pain: lessons from congenital insensitivity to pain with anhidrosis. *Clin Genet* **82**, 341-50 (2012).

103. Yozu, A. *et al.* Hereditary sensory and autonomic neuropathy types 4 and 5: Review and proposal of a new rehabilitation method. *Neurosci Res* **104**, 105-11 (2016).

104. Gupta, B. Congenital insensitivity of pain with anhidrosis. *Indian J Pediatr* **70**, 109-11 (2003).

105. Mardy, S. *et al.* Congenital insensitivity to pain with anhidrosis: novel mutations in the TRKA (NTRK1) gene encoding a high-affinity receptor for nerve growth factor. *Am J Hum Genet* **64**, 1570-9 (1999).

106. Capsoni, S. From genes to pain: nerve growth factor and hereditary sensory and autonomic neuropathy type V. *Eur J Neurosci* **39**, 392-400 (2014).

107. Einarsdottir, E. *et al.* A mutation in the nerve growth factor beta gene (NGFB) causes loss of pain perception. *Hum Mol Genet* **13**, 799-805 (2004).

108. Carvalho, O.P. *et al.* A novel NGF mutation clarifies the molecular mechanism and extends the phenotypic spectrum of the HSAN5 neuropathy. *J Med Genet* **48**, 131-5 (2011).

109. Kuruvilla, R. *et al.* A neurotrophin signaling cascade coordinates sympathetic neuron development through differential control of TrkA trafficking and retrograde signaling. *Cell* **118**, 243-55 (2004).

110. Houlden, H. *et al.* A novel TRK A (NTRK1) mutation associated with hereditary sensory and autonomic neuropathy type V. *Ann Neurol* **49**, 521-5 (2001).

111. Toscano, E., Simonati, A., Indo, Y. & Andria, G. No mutation in the TRKA (NTRK1) gene encoding a receptor tyrosine kinase for nerve growth factor in a patient with hereditary sensory and autonomic neuropathy type V. *Ann Neurol* **52**, 224-7 (2002).

112. Axelrod, F.B. Hereditary sensory and autonomic neuropathies. Familial dysautonomia and other HSANs. *Clin Auton Res* **12 Suppl 1**, I2-14 (2002).

113. Smeyne, R.J. *et al.* Severe sensory and sympathetic neuropathies in mice carrying a disrupted Trk/NGF receptor gene. *Nature* **368**, 246-9 (1994).

114. Crowley, C. *et al.* Mice lacking nerve growth factor display perinatal loss of sensory and sympathetic neurons yet develop basal forebrain cholinergic neurons. *Cell* **76**, 1001-11 (1994).

115. Edvardson, S. *et al.* Hereditary sensory autonomic neuropathy caused by a mutation in dystonin. *Ann Neurol* **71**, 569-72 (2012).

116. Ferrier, A. *et al.* Transgenic expression of neuronal dystonin isoform 2 partially rescues the disease phenotype of the dystonia musculorum mouse model of hereditary sensory autonomic neuropathy VI. *Hum Mol Genet* **23**, 2694-710 (2014).

117. Manganelli, F. *et al.* Novel mutations in dystonin provide clues to the pathomechanisms of HSAN-VI. *Neurology* **88**, 2132-2140 (2017).

118. Leipold, E. *et al.* A de novo gain-of-function mutation in SCN11A causes loss of pain perception. *Nat Genet* **45**, 1399-404 (2013).

119. Zhang, X.Y. *et al.* Gain-of-function mutations in SCN11A cause familial episodic pain. *Am J Hum Genet* **93**, 957-66 (2013).

120. Gold, M.S. & Gebhart, G.F. Nociceptor sensitization in pain pathogenesis. *Nat Med* **16**, 1248-57 (2010).

121. Dib-Hajj, S., Black, J.A., Cummins, T.R. & Waxman, S.G. NaN/Nav1.9: a sodium channel with unique properties. *Trends Neurosci* **25**, 253-9 (2002).

122. Saini, A.G. *et al.* Hereditary Sensory Polyneuropathy, Pain Insensitivity and Global Developmental Delay due to Novel Mutation in PRDM12 Gene. *Indian J Pediatr* **84**, 332-333 (2017).

123. Kinameri, E. *et al.* Prdm proto-oncogene transcription factor family expression and interaction with the Notch-Hes pathway in mouse neurogenesis. *PLoS One* **3**, e3859 (2008).

124. Chen, Y.C. *et al.* Transcriptional regulator PRDM12 is essential for human pain perception. *Nat Genet* **47**, 803-8 (2015).

125. Mead, S. & Reilly, M.M. A new prion disease: relationship with central and peripheral amyloidoses. *Nat Rev Neurol* **11**, 90-7 (2015).

126. Mead, S. *et al.* A novel prion disease associated with diarrhea and autonomic neuropathy. *N Engl J Med* **369**, 1904-14 (2013).

127. Wulf, M.A., Senatore, A. & Aguzzi, A. The biological function of the cellular prion protein: an update. *BMC Biol* **15**, 34 (2017).

128. Kherbaoui-Redouani, L. *et al.* Hereditary sensory neuropathy with spastic paraplegia. *Eur J Paediatr Neurol* **8**, 95-9 (2004).

129. Bouhouche, A., Benomar, A., Bouslam, N., Chkili, T. & Yahyaoui, M. Mutation in the epsilon subunit of the cytosolic chaperonin-containing t-complex peptide-1 (Cct5) gene causes autosomal recessive mutilating sensory neuropathy with spastic paraplegia. *J Med Genet* **43**, 441-3 (2006).

130. Nikawa, J. & Kimura, M. A novel function of the human chaperonin CCT epsilon subunit in yeast. *Biosci Biotechnol Biochem* **76**, 199-201 (2012).

131. Roddier, K. *et al.* Two mutations in the HSN2 gene explain the high prevalence of HSAN2 in French Canadians. *Neurology* **64**, 1762-7 (2005).

132. Hould, F. & Verret, S. [Hereditary radicular neuropathy with sensory loss: study of a French-Canadian family]. *Laval Med* **38**, 454-9 (1967).

133. Lessard, J.M. & Pouliot, A. [Morvan's disease]. *Laval Med* **18**, 1017-32 (1953).

134. Heller, I.H. & Robb, P. Hereditary sensory neuropathy. *Neurology* **5**, 15-29 (1955).

135. Dyck, P.J. Histologic measurements and fine structure of biopsied sural nerve: normal, and in peroneal muscular atrophy, hypertrophic neuropathy, and congenital sensory neuropathy. *Mayo Clin Proc* **41**, 742-74 (1966).

136. I, K. Hereditary Sensory and Autonomic Neuropathy Type II. in *GeneReviews™* (ed. Pagon RA, B.T., Dolan CR, et al., editors) (Seattle, USA, 2010).

137. Kurth, I. Hereditary Sensory and Autonomic Neuropathy Type II. in *GeneReviews(R)* (eds. Pagon, R.A. *et al.*) (Seattle (WA), 1993).

138. Yuan, J. *et al.* Hereditary sensory and autonomic neuropathy type IID caused by an SCN9A mutation. *Neurology* **80**, 1641-9 (2013).

139. Roddier, K. *et al.* Two mutations in the *HSN2* gene explain the high prevalence of HSAN2 in French Canadians. *Neurology* **in press**(2005).

140. Riviere, J.B. *et al.* A mutation in the HSN2 gene causes sensory neuropathy type II in a Lebanese family. *Ann Neurol* **56**, 572-5 (2004).

141. Cho, H.J., Kim, B.J., Suh, Y.L., An, J.Y. & Ki, C.S. Novel mutation in the HSN2 gene in a Korean patient with hereditary sensory and autonomic neuropathy type 2. *J Hum Genet* **51**, 905-8 (2006).

142. Coen, K. *et al.* Novel mutations in the HSN2 gene causing hereditary sensory and autonomic neuropathy type II. *Neurology* **66**, 748-51 (2006).

143. Wilson, F.H. *et al.* Human hypertension caused by mutations in WNK kinases. *Science* **293**, 1107-12 (2001).

144. Takagi, M. *et al.* New HSN2 mutation in Japanese patient with hereditary sensory and autonomic neuropathy type 2. *Neurology* **66**, 1251-2 (2006).

145. Yamada, K., Yuan, J., Mano, T., Takashima, H. & Shibata, M. Arthropathy-related pain in a patient with congenital impairment of pain sensation due to hereditary sensory and autonomic neuropathy type II with a rare mutation in the WNK1/HSN2 gene: a case report. *BMC Neurol* **16**, 201 (2016).

146. Levi-Montalcini, R. The nerve growth factor 35 years later. *Science* **237**, 1154-62 (1987).

147. Lu, B., Pang, P.T. & Woo, N.H. The yin and yang of neurotrophin action. *Nat Rev Neurosci* **6**, 603-14 (2005).

148. Spinosa, M.R. *et al.* Functional characterization of Rab7 mutant proteins associated with Charcot-Marie-Tooth type 2B disease. *J Neurosci* **28**, 1640-8 (2008).

149. Cogli, L., Piro, F. & Bucci, C. Rab7 and the CMT2B disease. *Biochem Soc Trans* **37**, 1027-31 (2009).

150. Houlden, H. *et al.* A novel RAB7 mutation associated with ulcero-mutilating neuropathy. *Ann Neurol* **56**, 586-90 (2004).

151. Cogli, L. *et al.* CMT2B-associated Rab7 mutants inhibit neurite outgrowth. *Acta Neuropathol* **120**, 491-501 (2010).

152. Li, G. & Marlin, M.C. Rab family of GTPases. *Methods Mol Biol* **1298**, 1-15 (2015).

153. Stenmark, H. & Olkkonen, V.M. The Rab GTPase family. *Genome Biol* **2**, REVIEWS3007 (2001).

154. Zerial, M. & McBride, H. Rab proteins as membrane organizers. *Nat Rev Mol Cell Biol* **2**, 107-17 (2001).

155. Zhang, M., Chen, L., Wang, S. & Wang, T. Rab7: roles in membrane trafficking and disease. *Biosci Rep* **29**, 193-209 (2009).

156. Riviere, J.B. *et al.* KIF1A, an axonal transporter of synaptic vesicles, is mutated in hereditary sensory and autonomic neuropathy type 2. *Am J Hum Genet* **89**, 219-30 (2011).

157. Rajasekharan, S., Martens, L., Domingues, L. & Cauwels, R. SCN9A channelopathy associated autosomal recessive Congenital Indifference to Pain. A case report. *Eur J Paediatr Dent* **18**, 66-68 (2017).

158. Chiabrando, D. *et al.* Mutations in the Heme Exporter FLVCR1 Cause Sensory Neurodegeneration with Loss of Pain Perception. *PLoS Genet* **12**, e1006461 (2016).

159. Shaibani, A., Wong, L.J., Wei Zhang, V., Lewis, R.A. & Shinawi, M. Autosomal recessive posterior column ataxia with retinitis pigmentosa caused by novel mutations in the FLVCR1 gene. *Int J Neurosci* **125**, 43-9 (2015).

160. Nizon, M. *et al.* ARL6IP1 mutation causes congenital insensivity to pain, self-mutilation and spastic paraplegia. *Clin Genet* (2017).

161. Yonekawa, Y. *et al.* Defect in synaptic vesicle precursor transport and neuronal cell death in KIF1A motor protein-deficient mice. *J Cell Biol* **141**, 431-41 (1998).

162. Okada, Y., Yamazaki, H., Sekine-Aizawa, Y. & Hirokawa, N. The neuron-specific kinesin superfamily protein KIF1A is a unique monomeric motor for anterograde axonal transport of synaptic vesicle precursors. *Cell* **81**, 769-80 (1995).

163. Gibson, D.G. *et al.* Enzymatic assembly of DNA molecules up to several hundred kilobases. *Nat Methods* **6**, 343-5 (2009).

164. Nesvizhskii, A.I., Keller, A., Kolker, E. & Aebersold, R. A statistical model for identifying proteins by tandem mass spectrometry. *Anal Chem* **75**, 4646-58 (2003).

165. Lippincott, J. & Apostol, I. Carbamylation of cysteine: a potential artifact in peptide mapping of hemoglobins in the presence of urea. *Anal Biochem* **267**, 57-64 (1999).

166. Costantini, L.M., Fossati, M., Francolini, M. & Snapp, E.L. Assessing the tendency of fluorescent proteins to oligomerize under physiologic conditions. *Traffic* **13**, 643-9 (2012).

167. Nolles, A. *et al.* Encapsulation into complex coacervate core micelles promotes EGFP dimerization. *Phys Chem Chem Phys* **19**, 11380-11389 (2017).

168. Wang, C. *et al.* Synaptotagmin-11 inhibits clathrin-mediated and bulk endocytosis. *EMBO Rep* **17**, 47-63 (2016).

169. Xie, Z. *et al.* Molecular Mechanisms for the Coupling of Endocytosis to Exocytosis in Neurons. *Front Mol Neurosci* **10**, 47 (2017).

170. Koo, S.J. *et al.* Vesicular Synaptobrevin/VAMP2 Levels Guarded by AP180 Control Efficient Neurotransmission. *Neuron* **88**, 330-44 (2015).

171. Leitz, J. & Kavalali, E.T. Ca2+ Dependence of Synaptic Vesicle Endocytosis. *Neuroscientist* **22**, 464-76 (2016).

172. Saheki, Y. & De Camilli, P. Synaptic vesicle endocytosis. *Cold Spring Harb Perspect Biol* **4**, a005645 (2012).

173. Gustavsson, N. & Han, W. Calcium-sensing beyond neurotransmitters: functions of synaptotagmins in neuroendocrine and endocrine secretion. *Biosci Rep* **29**, 245-59 (2009).

174. Dean, C. *et al.* Synaptotagmin-IV modulates synaptic function and long-term potentiation by regulating BDNF release. *Nat Neurosci* **12**, 767-76 (2009).

175. Mao, Y., Chen, J., Maynard, J.A., Zhang, B. & Quiocho, F.A. A novel all helix fold of the AP180 amino-terminal domain for phosphoinositide binding and clathrin assembly in synaptic vesicle endocytosis. *Cell* **104**, 433-40 (2001).

APPENDIX

Table S1: List of the proteins identified by mass spectrometry analysis of KIF1A/25B

Accession Number (Mouse)	Protein	Size (kDa)
VATB2	V-type proton ATPase subunit B, brain isoform OS=Mus musculus GN=Atp6v1b2 PE=1 SV=1	57
A3KGL7	Ribosomal protein S6 kinase polypeptide 1 OS=Mus musculus GN=Rps6ka1 PE=4 SV=1	82
MAP4	Microtubule-associated protein 4 OS=Mus musculus GN=Map4 PE=1 SV=3	117
Q8BH80	Vesicle-associated membrane protein, associated protein B and C OS=Mus musculus GN=Vapb PE=2 SV=1	27
ATP5J	ATP synthase-coupling factor 6, mitochondrial OS=Mus musculus GN=Atp5j PE=1 SV=1	12
DNJA1	DnaJ homolog subfamily A member 1 OS=Mus musculus GN=Dnaja1 PE=1 SV=1	45
Q58EA6	MCG10725, isoform CRA_a OS=Mus musculus GN=Rps25 PE=2 SV=1	14
COX6C	Cytochrome c oxidase subunit 6C OS=Mus musculus GN=Cox6c PE=1 SV=3	8

Accession Number (Mouse)	Protein	Size (kDa)
GLNA	Glutamine synthetase OS=Mus musculus GN=Glul PE=1 SV=6	42
ATP5I	ATP synthase subunit e, mitochondrial OS=Mus musculus GN=Atp5i PE=1 SV=2	8
Q58EW0	Ribosomal protein L18 OS=Mus musculus GN=Rpl18 PE=2 SV=1	22
S12A2	Solute carrier family 12 member 2 OS=Mus musculus GN=Slc12a2 PE=1 SV=1	131
Q3TK12	Putative uncharacterized protein OS=Mus musculus GN=Rps17 PE=2 SV=1	16
H4	Histone H4 OS=Mus musculus GN=Hist1h4a PE=1 SV=2	11
AP180	Clathrin coat assembly protein AP180 OS=Mus musculus GN=Snap91 PE=1 SV=1	92
GSK3B	Glycogen synthase kinase-3 beta OS=Mus musculus GN=Gsk3b PE=1 SV=2	47
Q3UDZ1	Ras homolog gene family, member G OS=Mus musculus GN=Rhog PE=2 SV=1	21

Accession Number (Mouse)	Protein	Size (kDa)
Q3TI27	Ribose-phosphate pyrophosphokinase OS=Mus musculus GN=Prps1 PE=2 SV=1	35
Q3TPH5	Putative uncharacterized protein OS=Mus musculus GN=Syt11 PE=2 SV=1	48
KC1E	Casein kinase I isoform epsilon OS=Mus musculus GN=Csnk1e PE=1 SV=2	47
Q3TK73	Putative uncharacterized protein OS=Mus musculus GN=Rpl7 PE=2 SV=1	31
SNW1	SNW domain-containing protein 1 OS=Mus musculus GN=Snw1 PE=1 SV=3	61
KIF3A	Kinesin-like protein KIF3A OS=Mus musculus GN=Kif3a PE=1 SV=1	80
MAZ	Myc-associated zinc finger protein OS=Mus musculus GN=Maz PE=1 SV=1	49
Q3U781	MCG21131, isoform CRA_a OS=Mus musculus GN=Srsf3 PE=2 SV=1	14
Q3TKD1	MCG17786, isoform CRA_a OS=Mus musculus GN=Rfc3 PE=2 SV=1	41

Accession Number (Mouse)	Protein	Size (kDa)
68MP	6.8 kDa mitochondrial proteolipid OS=Mus musculus GN=Mp68 PE=2 SV=1	7
Q3U561	Ribosomal protein OS=Mus musculus GN=Rpl10a PE=2 SV=1	25
RS7	40S ribosomal protein S7 OS=Mus musculus GN=Rps7 PE=2 SV=1	22
A0AUV1	Histone H2A (Fragment) OS=Mus musculus GN=Hist1h2ah PE=2 SV=1	14
KC1A	Casein kinase I isoform alpha OS=Mus musculus GN=Csnk1a1 PE=2 SV=2	39
TOP1	DNA topoisomerase 1 OS=Mus musculus GN=Top1 PE=1 SV=2	91
1433G	14-3-3 protein gamma OS=Mus musculus GN=Ywhag PE=1 SV=2	28
Q3TET0	Putative uncharacterized protein OS=Mus musculus GN=Cct7 PE=2 SV=1	60
Q8BP43	Tropomyosin 1, alpha, isoform CRA_c OS=Mus musculus GN=Tpm1 PE=2 SV=1	33

Accession Number (Mouse)	Protein	Size (kDa)
A2AJH9	Microtubule-associated protein 7 domain containing 1 (Fragment) OS=Mus musculus GN=Mtap7d1 PE=4 SV=1	65
Q8BKG0	Transporter (Fragment) OS=Mus musculus GN=Slc6a11 PE=2 SV=1	66
Q925S1	MRP5 (Fragment) OS=Mus musculus GN=Gm7175 PE=2 SV=1	12